COMPRESSIBILITY EFFECTS IN MODELING TWO-PHASE LIQUID DOMINATED GEOTHERMAL RESERVOIRS

4

A Report

Submitted to the Department of Petroleum Engineering

of Stanford University

in Partial Fulfillment of the Requirements for the

Degree of Master of Science

by

David C. Brock

June, 1986.

ABSTRACT

The use of the Hurst Simplified Model to history match the drawdown behavior of liquid dominated geothermal reservoirs is studied. Liquid dominated reservoirs virtually always have a region of intimately mixed vapor and liquid (two-phase zone). Such regions have high compressibilities **up** to three orders of magnitude greater than that of liquid only. It is therefore important that a reservoir model remains valid over a large range of compressibilities, and that it not require reservoir compressibility as an input parameter.

The Hurst Simplified Model, linear and radial geometries, is formulated for use in liquid dominated geothermal reservoirs. The model is tested on drawdown histories of five reservoirs (Ahuachapan, Broadlands, Ellidaar, Svartsengi, and Wairakei) spanning a large range of compressibilities. The matches yielded reasonable compressibilities and fits to histories in most cases, with the fields at either compressibility extreme introducing only slight problems.

i

ACKNOWLEDGEMENT

The author wishes to thank Professor Jon S. Gudmundsson, principal advisor of this research, for his invaluable guidance. Thanks also to the students, faculty, and staff of the Department of Petroleum Engineering at Stanford University, particularly Professor Roland N. Horne, for their support.

TABLEOFCONTENTS

LIST OF FIGURES

LIST OF TABLES

1. INTRODUCTION

When producing a geothermal reservoir, it is important to be able to predict the drawdown behavior of the reservoir. Many theoretical and empirical models exist, but even the simplest generally require information on reservoir geometry (shape, dimensions), flow characteristics (porosity, permeability), and fluid properties (viscosity). Further, most commercial fields have recharge of reservoir fluids, meaning that characteristics of the supporting aquifer are also needed. In practical applications, many of these parameters are not known and their values must be assumed. Through history matching, some of those unknowns may be determined.

Water influx models in use are of two types: numerical and lumped parameter. The numerical model involves dividing the reservoir into blocks, assigning values (of permeability and porosity, for example) to each block, and solving the flow equations in finite difference form. Note that much reservoir data, such as Permeability and porosity distributions and geometry is necessary to use this type of model.

Lumped parameter models are solutions of the flow equations for simplified situations which are then assumed applicable to various real situations. Water influx methods originating in the petroleum industry (e.g. Hurst (1958) and Schilthuis (1936)) fall into this category and are applicable to geothermal reservoirs (Olsen, 1984). The advantage to Lumped parameter methods is that less reservoir information is necessary, and that some reservoir information may be obtained through history matching.

The Hurst Simplified Model (Hurst, 1958) is widely used in the petroleum industry. This study examines its use in geothermal situations where some of the system parameters are not known. The following questions are investigated:

1. How is the Hurst Simplified model applied to geothermal systems?
2. Of the reservoir parameters, which must be accurately known for successful modeling? In practical situations, what values are usually known or are easily estimable?
3. What is the effect of compressibility in lumped parameter reservoir modeling?
4. What information can a Hurst model history match reveal?
5. Can the Hurst model be applied to any general situation, or is it limited strictly to the specific geometry for which it is derived ?
6. Is either of the formulations (linear or radial) of the Hurst model more accurate or convenient?

The focus of this report is on the modeling of geothermal reservoirs using a method developed for oil reservoirs. In doing so, it seems that the thermodynamics of the geothermal reservoir are being ignored. But while thermodynamics is not implicitly part of the depletion model, a knowledge of the thermodynamics of the liquid dominated geothermal reservoir is needed to explain and interpret the results of the modeling. Whiting and Ramey (1969) and Donaldson et al. (1983) discuss the thermodynamics of geothermal systems, the former focusing on production engineering, the latter on reservoir description. Further models of geothermal reservoir thermodynamics are those of Brigham and Morrow (1977) and Martin (1975).

A few authors have reviewed the use of water influx models for geothermal modeling. Olsen (1985) compares numerous models using the Svartsengi reservoir as an example. Fradkin et al. (1981) compare models using data from Wairakei. A more general review of models is that of Grant (1983). Among water influx models in the petroleum literature are those of Schilthuis (1949), Hurst (1958), Carter and Tracy (1960), Fetkovitch (1971), and Allard and Chen (1984). Studies and models of specific geothermal fields include Gudmundsson and Olsen (1985), Gudmundsson et al. (1984), and Regaldo (1981) for Svartsengi; Hitchcock and Bixley (1976) for Broadlands; Atkinson et al. (1978) for Bagnore; and Brigham and Neri (1980) for Lardarello.

2. THERMODYNAMICS OF GEOTHERMAL RESERVOIRS

The thermodynamics of geothermal reservoirs are discussed by several authors (Whiting and Ramey, 1969; Martin, 1975; and Grant et al., 1982). Contained here is just enough general thermodynamics to allow discussion of two-phase zones and two-phase compressibilities.

2.1 Temperature Profiles

The highest temperature at which liquid may exist is given by the vapor pressure or boiling curve of the liquid. If the liquid has a hydrostatic pressure profile, deeper portions are at higher pressure and have a higher boiling point. Figure 1 is a vapor pressure (pressure vs. temperature) curve for pure water. Turned on its side, it can become a temperature vs. depth diagram. Often geothermal reservoirs will have this temperature distribution, called the boiling-point-for-depth (BPD) temperature profile.

Generally, geothsrmal reservoirs are subject to upflow (Donaldson et al., 1983): hotter fluids flow upward and carry heat by convection. In such a convective environment, temperature is close to constant and linear with depth, at least as long as the temperature remains less than the boiling point.

Thus a generalized geothermal reservoir description could be a temperature distribution which is linear at depth due to convection, then follows the boiling point curve at the top of the reservoir. Figure 2 shows temperature vs. depth data from the Svartsengi field in Iceland which exhibits this composite behavior.

2.2 Two-Phase Zones

Consider a liquid reservoir whose initial temperature distribution is a composite of BPD at the top, and linear at depth, as just discussed. When such a reservoir is produced, pressure drops, the boiling point decreases, so the portion of the reservoir that lies on the boiling curve begins to boil. More of what was previously the linear convective profile now lies along the boiling curve (Figure 3). When boiling occurs, a two-phase zone is created.

A more in-depth discussion of the formation of two-phase zones is not necessary for our purposes. The above discussion is meant to give a qualitative feel for how and why two-phase zones exist in geothermal reservoirs. Treatments that discuss phase mobilities and gravity segregation include Martin (1975) and Donaldson et al. (1983).

Boiling may occur due to production, resulting in a two-phase zone; that is, a zone of mixed steam and water. Confirming this, Grant (1981) states that nearly all high-temperature fields contain a two-phase zone, maintained in spite of gravity segregation. This is important because, as will be shown, the compressibility of a two-phase mixture is radically different than that of either phase alone.

2.3 Compressibility

The isothermal compressibility relates the change of volume of a fluid due to change in pressure under isothermal conditions. Petroleum reservoirs are almost always isothermal systems. Temperature decline in geothermal systems is so gradual that they may be approximated as isothermal. The isothermal compressibility (hereafter refered to simply as compressibility) of water and steam are available.

Compressibility c is defined:

$$c \equiv -\frac{1}{V}\frac{dV}{dP} \tag{1}$$

The compressibility of a substance may be calculated from isotherms on a P-V diagram of the substance. The compressibility is related to the inverse of the slope of the isotherm.

Figures 4 and 5 are sample P-V diagrams for a pure substance and a mixture (Macias-Chapa, 1985). The isotherms in the liquid region are much steeper than those in the vapor region, which are in turn steeper than those in the two-phase region. Thus, liquid compressibilities are smaller than gas compressibilities, while two-phase compressibilities are greater than either liquid or vapor alone. For water at 240 °C, the liquid compressibility is $1.2\times10^{-9}Pa^{-1}$, while the vapor compressibility is greater: $3.0\times10^{-7}Pa^{-1}$ (Grant et al., 1982).

While the concept of compressibility normally implies a confined system, an unconfined compressibility arising from a rising or falling water level can also be computed. This is a real situation as many geothermal reservoirs communicate, through fractures, to the surface and may thereby be nearly unconfined. Consider a porous medium of area **A,** porosity φ, and height h. Adding a volume of liquid dV causes the level to rise by dh, and the pressure to rise by ρ g dh. Compressibility c is defined

$$c \equiv -\frac{1}{V}\frac{dV}{dP} \tag{1}$$

where

$$V = Ah$$

$$dV = -A\varphi dh$$

$$dP = \rho g dh$$

Substituting into **Eq.** 1,

$$c = \frac{1}{Ah}\frac{A\varphi dh}{\rho g dh} \tag{2}$$

$$c = \frac{\varphi}{\rho g h} \tag{3}$$

Considering an aquifer 500 m thick with 15% porosity, at 240 $^\circ C$, the compressibility is

$$c = 3.8\times10^{-8}\ Pa^{-1}$$

(Grant et al., 1982)

Consider liquid water and steam in equilibrium in a porous medium. A small reduction in pressure causes a large increase in volume because some of the liquid will vaporize into steam. The rock must cool to supply the heat of vaporization, so the rock thermal properties affect the system compressibility. Grant and Sorey (1979) give the following derivation.

As long as two phases exist in the system, the presure and temperature are related by the vapor pressure curve. If pressure drops by ΔP, the temperature change ΔT is

$$\Delta T = \frac{\Delta P}{(dP/dT)_{sat}} \tag{4}$$

The heat released by the rock as its temperature drops by ΔT is

$$Q_{thermal} = V(\rho C)_T \Delta T \tag{5}$$

where

$$(\rho C)_T = (1-\varphi)\rho_m C_m + \varphi S_w \rho_w C_w \tag{6}$$

This heat is used to vaporize the water. The resulting change in volume is

$$\Delta V = \frac{V(\rho C)_T \Delta T}{H_{latent}}\left(\frac{1}{\rho_s} - \frac{1}{\rho_w}\right) \tag{7}$$

Using Eq. 2 and 5 in Eq. 1, the two-phase compressibility c_T is

$$c_T = \frac{1}{\varphi}\frac{(\rho C)_T}{H_{latent}}\frac{\rho_w - \rho_s}{\rho_w \rho_s}\left(\frac{dT}{dS}\right)_{sat} \tag{8}$$

A two-phase mixture at $240\,^\circ C$, 15% porosity, and $(\rho C)_T = 2.5\,MJ/m^3K$, the compressibility is $1.4\times10^{-6}\,Pa^{-1}$

The compressibilities observable in geothermal reservoirs have a large range. Recall and compare the values arrived at above:

$$
\begin{array}{rl}
\textit{confined } \textbf{water} & c = 1.2\times 10^{-9}\ Pa^{-1} \\
\textit{unconfined } \textbf{water} & c = 3.8\times 10^{-8}\ Pa^{-1} \\
\textit{confined } \textbf{steam} & c = 3.0\times 10^{-7}\ Pa^{-1} \\
\textit{confined } \text{two} \textbf{-phase} & c = 1.4\times 10^{-6}\ Pa^{-1}
\end{array}
$$

Compressibilities of geothermal fluids can thus range over three orders of magnitude.

The analyses just done were concerned mainly with the compressibilities of the fluids themselves. Geothermal reservoirs consist of compressible fluids in a compressible porous medium. The total system compressibility is given by

$$c_T = c_w + c_f \tag{9}$$

where c_f is the formation compressibility. Craft and Hawkins (1959) state that formation compressibilities range from $4.3\times10^{-10} Pa^{-1}$ to $15\times10^{-10} Pa^{-1}$. These are of the order of the compressibility of liquid water. Ramey (1964) states that the total compressibility is the correct compressibility to use in modeling.

2.4 Other Variables

Other reservoir and fluid parameters used in the water influx modeling are viscosity μ, permeability k, porosity φ, and fluid density ρ. In most cases, values of these are known from tests, or reasonable values can be inferred. For example, experience shows that reasonable values of φ might range from 5 to 20%. Values for **k** might range from 1 to 100 mD , but approximate values usually exist from well tests. The variability of some of the parameters used in the Hurst analysis are compared in Figure **6,** which shows the range (in orders of magnitude) of these reasonable values for the parameters.

Compressibility easily has the largest range, the compressibility depending on the extent of the two-phase zone. The extent of the two-phase zone in a geothermal reservoir is generally not known (Donaldson et al., 1983). Thus, a useful model for the reservoir is one which does not have compressibility as an input parameter but instead computes and outputs it. The Hurst model as formulated and used in this report determines compressibility through a history match. Then from this compressibility, an idea of the existence and extent of two-phase zone may be inferred.

3. WATER INFLUX MODELING

There are two general categories of reservoir models: numerical simulations and lumped parameter models. In numerical simulation, the reservoir system is divided into small blocks, each block having its own properties, and finite difference forms of the governing equations are used to calculate the time and space variation of, for example, pressure in the reservoir. In lumped-parameter models, average values of fluid and flow properties are assumed throughout the reservoir, and analytic solutions are derived.

Lumped-parameter models are generally the method of choice. Numerical methods demand much computer time and more input information than is generally known. For example, a lumped parameter model uses an average porosity and permeability, while a numerical model requires porosities and permeabilities for each block, which are unlikely to be known. Although lumped parameter models assume average properties and regular geometries, they are useful and accurate in many practical situations, and easy to use.

A lumped parameter model is a material balance on a closed reservoir: producing an amount of fluid causes a pressure drop in the reservoir. Both oil and geothermal fields are often connected to a supporting aquifer, however, which adds an influx term to the material balance. Many authors in the petroleum literature have modeled this situation for different geometries and conditions: Schilthuis (1949), Hurst (1958), and Fetkovitch (1971). Olsen (1984) tested all of these models on data from the Svartsengi geothermal field.

These models address flow from an aquifer more or less horizontally adjacent to the reservoir ("edge-water drive"). Allard and Chen (1984) did a numerical simulation of "bottom-water drive", noting that edge-water models do not accurately model bottom water situations as the ratio of reservoir thickness to reservoir radius increases.

3.1 Hurst Simplified Method

A commonly used water influx model is the Hurst Simplified Method (Hurst, 1956). It treats edge-water drive in linear and radial cases. The method takes a material balance on the reservoir and applies the solution of the diffusivity equation in Laplace space (Van Everdingen and Hurst, 1949) to account for water influx from the aquifer. The "simplification" is that by using the Laplace transformation, an expression for drawdown as an explicit function of production rate and time is found. A parameter containing the ratio of aquifer to reservoir compressibility is central to this derivation.

Hurst's paper develops the method for use in oil reservoir-aquifer systems. It is easily adapted for use in geothermal reservoir systems by using hot geothermal fluid properties in place of oil properties in the Hurst formulation. Olsen (1964) rederived the Hurst linear model for geothermal applications. Because the derivation is often neglected, and to identify some important points in the use of the method, the Hurst derivations for both linear and radial cases will now be given.

3.1.1 Linear Model Derivation

The material balance on the geothermal reservoir is written

$$W = W_i - W_p + W_e \tag{10}$$

(Mass of water in the reservoir equals the initial mass, less produced mass, plus encroached mass.) For a confined system, masses W and W_i are simply related to the reservoir volume:

$$W = V\varphi\rho \tag{11}$$

so that Eq. 10 becomes

$$V\varphi(\rho - \rho_i) = -W_p + W_e \tag{12}$$

The difference in densities may be approximated

$$\rho - \rho_i = \int_0^t \frac{d\rho}{dt} dt \tag{13}$$

$$\rho - \rho_i = \int_{P_i}^{P} \frac{d\rho}{dP} \frac{dP}{dt} dt \tag{14}$$

The isothermal compressibility is written

$$c = \frac{1}{\rho} \frac{d\rho}{dP} \tag{15}$$

Substituting Eq. 15 into Eq. **14,**

$$\rho - \rho_i = \int_{P_i}^{P} c \rho dP \tag{16}$$

$$\rho - \rho_i = c \rho_{av} (P - P_i) \tag{17}$$

Substituting into the material balance (Eq. 12)

$$V \varphi c \rho_{av} (P - P_i) = -W_p + W_e \tag{18}$$

Assuming constant production rate,

$$W_p = w_p t \tag{19}$$

and writing drawdown

$$P_i - P = \Delta P \tag{20}$$

Eq. 18 becomes

$$-V \varphi c \rho_{av} \Delta P = W_e - w_p t \tag{21}$$

The cumulative water influx **is** written as the convolution integral:

$$W_e = B \int_0^{t_D} \frac{d\Delta P}{dt_D^*} Q_D(t_D - t_D^*) dt_D^* \tag{22}$$

where dimensionless time is defined

$$t_D \equiv \frac{k_a t}{\varphi \mu_a c_a L_a^2} \tag{23}$$

In the infinite aquifer, L is assigned unit length. Substituting Eq. 22 and 23 into 21.

$$-V\varphi c_r \rho_r \Delta P \;=\; B\int_0^{t_D} \frac{d\Delta P}{dt_D^*} Q_D(t_D - t_D^*)dt_D^* \;-\; \frac{w_p t_D \varphi \mu_a c_a L_a^2}{k_a} \tag{24}$$

The Laplace transform of Eq. 24 is

$$-V\varphi \rho_r c_r \overline{\Delta P} \;=\; Bs\overline{\Delta P}\overline{Q_D} \;-\; \frac{\varphi \mu_a c_a L_a^2 w_p}{k_a s^2} \tag{25}$$

For the infinite linear aquifer geometry, the influx function $\overline{Q_D}$, as a result of the LaPlace space solution of the diffusivity equation (van Everdingen and Hurst, 1949) is written

$$\overline{Q_D} = s^{-3/2} \tag{26}$$

and

$$B = A\varphi c_a \rho_a \tag{27}$$

Substituting Eq. 26 and 27 into 25,

$$A\varphi c_a \rho_a s \overline{\Delta P} s^{-3/2} + V\varphi \rho_r c_r \overline{\Delta P} = \frac{\varphi \mu_a c_a w_p}{k_a s^2} \tag{28}$$

Solving Eq. 28 for $\overline{\Delta P}$:

$$\overline{\Delta P} = \frac{\mu_a c_a w_p}{k_a A l c_r \rho_r s^{3/2}\left[\dfrac{c_a \rho_a}{l c_r \rho_r} + s^{1/2}\right]} \tag{29}$$

Defining the Hurst parameter λ

$$\lambda \equiv \frac{c_a \rho_a}{l c_r \rho_r} \tag{30}$$

Eq. 29 becomes

$$\overline{\Delta P} = \frac{\mu_a w_p \lambda}{k_a A \rho_a}\left[\frac{1}{s^{3/2}\,(\lambda + s^{1/2})}\right] \tag{31}$$

Inverting Eq. 31 to real space,

$$\Delta P = \frac{\mu_a w_p}{k_a A \rho_a \lambda}\left[e^{\lambda^2 t_D} erfc\,(\lambda t_D^{1/2}) - 1 + \frac{2\lambda t_D^{1/2}}{\pi^{1/2}}\right] \tag{32}$$

Eq. *32* may be superposed to account for changing flow rates:

$$\Delta P = \frac{\mu_a \lambda}{k_a A \rho_a}\sum w_p \; M\left[\lambda, (t_D - t_{D\,j})\right] \tag{33}$$

where

$$M[\lambda, t_D] = \frac{1}{\lambda^2}\left[e^{\lambda^2 t_D} erfc\,(\lambda t_D^{1/2}) - 1 + \frac{2\lambda t_D^{1/2}}{\pi^{1/2}}\right] \tag{34}$$

Equation **33** is explicit for ***AP,*** and is in real space. Other water influx methods previous to Hurst were not explicit in ***AP.*** As soon will be shown, the radial model is explicit in ***AP,*** but is not analytically invertible to real space.

An important thing to note is the form of the constant λ: a ratio of compressibilities and densities and a geometry term. It was commented earlier that the reservoir compressibility is an important value to determine, so it is important that we can calculate it from λ. In the next section, λ will be compared to the analogous parameter σ, which has no geometric term.

3.1.2 Radial Model Derivation

The previous derivation **is** unchanged for the radial case through Eq. 22. For the radial case, dimensionless time is defined as follows:

$$t_D = \frac{kt}{\varphi \mu c r_r^2} \tag{35}$$

where the r is reservoir radius.

One may question why in the infinite linear case the characteristic length was taken as unity, whereas in the radial case an actual physical dimension is used. The dimensionless time is used in the W_p term, the term describing the flow from the aquifer. In the linear case, a linear aquifer of infinite extent, there is no characteristic length. (The length of the reservoir is irrelevant to the aquifer.) But in the radial case, the reservoir radius is a characteristic length for the aquifer as it describes the inner radics of aquifer flow.

Continuing as before,

$$-V\varphi c_r \rho_r \Delta P = B\int_0^{t_D} \frac{d\Delta P}{dt_D} Q_D(t_D - t_D^*)dt_D - \frac{w_p t_D \varphi \mu_a c_a r_r^2}{k_a} \tag{36}$$

In Laplace space:

$$-V\varphi \rho_r c_r \overline{\Delta P} = Bs\,\overline{\Delta P}\,\overline{Q_D} - \frac{\varphi \mu_a c_a r_r^2 w_p}{k_a s^2} \tag{37}$$

For the radial case, the dimensionless influx 'unction is

$$\overline{Q_D} = \frac{K_1(\sqrt{s}\,)}{s^{3/2}K_0(\sqrt{s}\,)} \tag{38}$$

and the influx constant is

$$B = 2\pi r_r^2 \varphi c_a \rho_a h \tag{39}$$

Substituting Eq. **38** and **39** into 37,

$$\overline{\Delta P}\left[\frac{c_r\rho_r\sqrt{s}K_0(\sqrt{s}\,) + 2c_a\rho_a K_1(\sqrt{s}\,)}{\sqrt{s}K_0(\sqrt{s}\,)}\right] = \frac{\mu_a c_a w_p}{\pi k_a h s^2} \tag{40}$$

$$\overline{\Delta P} = \frac{\mu_a c_a w_p}{\pi k_a h s^{3/2} c_r \rho_r}\;\frac{K_0(\sqrt{s}\,)}{\sqrt{s}K_0(\sqrt{s}\,) + 2\dfrac{c_a\rho_a}{c_r\rho_r}K_1(\sqrt{s}\,)} \tag{41}$$

Defining the radial Hurst parameter σ:

$$\sigma \equiv 2\frac{c_a\rho_a}{c_r\rho_r} \tag{42}$$

Substituting into **Eq.** 41,

$$\overline{\Delta P} = \frac{\mu_a \sigma w_p}{2\pi k_a h \rho_a} \frac{K_0(\sqrt{s}\,)}{s^{3/2}\left[\sigma K_1(\sqrt{s}\,) + \sqrt{s}\, K_0(\sqrt{s}\,)\right]} \tag{43}$$

In real space,

$$\Delta P = \frac{\mu_a w_p \sigma}{2\pi k_a h \rho_a} N(\sigma, t_D - t_{D\,j}) \tag{44}$$

where

$$N(\sigma, t_D) = L^{-1}\left[\frac{K_0(\sqrt{s}\,)}{s^{3/2}[\sigma K_1(\sqrt{s}\,) + \sqrt{s}\, K_0(\sqrt{s}\,)]}\right] \tag{45}$$

As before, **Eq. 44** may be written in superposition form for varying rate:

$$\Delta P = \frac{\mu_a \sigma}{2\pi k_a h \rho_a} \sum \Delta w_p \; N(\sigma, t_D - t_{D\,j}) \tag{46}$$

Again, the expression is convenient as it is explicit in **AP.** However, in this case the Hurst function is not analytically invertible to real space. Numerical methods can be used to invert the function; the Stehfest algorithm is a suitable method.

A special case of the general radial solution is the solution for large *u*. In the limit, the drawdown is

$$\Delta P = \frac{\mu_a}{2\pi k_a h \rho_a} \sum \Delta w_p \; p_D(t_D - t_{D\,j}) \tag{47}$$

where $p_D(t_D)$ is the familiar line source solution (Earlougher, 1977)

$$p_D(t_D) = -\frac{1}{2} Ei \left[\frac{-1}{4t_D}\right] \tag{48}$$

Eq. 48 may be approximated

$$p_D(t_D) = \frac{1}{2}[\ln(t_D) + .80907] \tag{49}$$

when (approximately) $t_D > 5$.

The physical interpretation of using the line source solution is that the reservoir is small compared to the aquifer, so that the reservoir response is negligible compared to the aquifer drawdown response.

The Hurst radial parameter σ is a ratio of compressibilities and densities only. (The linear parameter A had a geometric term as well.) Good estimates or values for aquifer compressibility and density as well as reservoir liquid density usually are known. Therefore, once σ is found (through the history match), reservoir compressibility may be found without direct geometric information. In the radial case, the geometric information is contained in the dimensionless time term. In this way compressibility is a less strong function of the geometric term in the radial case than in the linear case.

4. MODEL APPLICATION

4.1 History Matching Method

The history matching scheme used in this report is that used by Olsen (1984) and Marcou (1985). The computer programs used in this report are modifications of programs used by those authors.

Recall the general Hurst model equation for the linear case:

$$\Delta P = \frac{\mu_a \lambda}{k_a A \rho_a} \sum_{j=1}^{n} \Delta w_p \; M\left[\lambda, (t_D - t_{D\,j})\right] \tag{33}$$

where

$$M[\lambda, t_D] = \frac{1}{\lambda^2}\left[e^{\lambda^2 t_D} erfc\,(\lambda t_D^{1/2}) - 1 + \frac{2\lambda t_D^{1/2}}{\pi^{1/2}}\right] \tag{34}$$

The data (history) consists of values of Ah, t, and w_j. We generally have a value or an estimate of the other reservoir and fluid constants, but not *h*. Define

$$x(k) = \sum_{j=1}^{k} \Delta w_j \; M\left[\lambda, (t_D - t_{D\,j})\right] \tag{50}$$

$$y(k) = \frac{AP}{\rho g} = \Delta h_k \tag{51}$$

A plot of **x**(n) vs y(n) will be linear for a system which fits the Hurst Model. Using data, a linear least squares regression on these **x** and y yields a slope, a_{lin}, which from **Eq.** 33 is

$$a_{lin} = \frac{\mu_a}{k A \rho_a \rho_r g} \lambda \tag{52}$$

All of these equations depend on λ, which is unknown. Thus, λ must first be guessed, the least squares fit done, the Hurst model drawdown calculated, and a standard deviation between the data and the Hurst model found. Another λ is chosen, and the process is repeated. The λ (and its a_{lin}) that minimizes the standard deviation is the correct reservoir parameter

In the radial case, the general procedure is nearly identical. However in the radial case, the Hurst function, **N**, is not. given analytically in real space:

$$N(\sigma,t_D) = L^{-1}\left[\frac{K_0(\sqrt{s}\,)}{s^{3/2}\left[\sigma K_1(\sqrt{s}\,) + \sqrt{s}\,K_0(\sqrt{s}\,)\right]}\right] \tag{45}$$

Because the history match is being done in the computer, a numerical method such as the Stehfest Algorithm (Stehfest, 1970) can be used to invert the equation.

The history match method for the radial model is identical to the linear case. Recall **Eq.** *50:*

$$\Delta P = \frac{\mu_a \sigma}{2\pi h k_a \rho_a} \sum_{j=1}^{n} \Delta w_p \; N(\sigma,t_D - t_{D\,j}) \tag{50}$$

As before, define

$$x(n) = \sum_{j=1}^{n} \Delta w_j \;\sigma\, N(\sigma,t_D - t_{D\,j}) \tag{53}$$

$$y(n) = \frac{AP}{\rho g} = \Delta h_n \tag{54}$$

The slope, a_{rad}, from the least squares fit is:

$$a_{rad} = \frac{\mu_a}{2\pi k h_a \rho_a \rho_r g}$$

As explained previously, values for σ and a_{rad} will result from the history match. Compressibility can then be determined from σ and the permeability-thickness product can be determined from a_{rad}.

In his paper, Hurst(1958) states that large radial systems can be modeled **as** linear systems. When looking at only early data, any system appears "large" (its boundaries are not felt), so the linear analysis should work. Thus, if a linear analysis works on the early data only, the system is probably radial.

In some cases, a linear fit could not be obtained; there was no minimum in the graph of standard deviation vs X. In these cases however, a linear fit could be obtained by using only the early data. This phenomenon indicates that the reservoir is of radial geometry.

4.2 Computer Application

The FORTRAN 77 computer codes used in this report are given, with details, in Appendix **A.** The algorithms are basically as described in Section 4.1. For each of the geometries (radial and linear) there are two programs: one to find the standard deviation and least-squares slope for a given σ or X, and one which prepares the model and actual drawdown graphs for a given σ or X and least-squares slope.

In the radial case, recall that the Hurst function is not given analytically in real space, so must be numerically inverted using the Stehfest Algorithm. Although the Stehfest Algorithm is well behaved in this application, it is slow. In this history match method, $x(k)$ and $y(k)$ are calculated for each k from one to n (the number of data points, often in the hundreds), and each $x(k)$ has a summation from one to k. The Hurst function is inside a doubly nested loop. For a data history of 200 points, the Hurst function is evaluated over twenty thousand times. Thus, to speed execution time, it was investigated whether a simple real-space approximation for the Hurst function could be obtained for the ranges of σ and t_D encountered in geothermal applications.

In the history match, recall that a σ is chosen, then all the data fit to yield a slope and a standard deviation. Thus, the Hurst function N was graphed vs a range of t_D's for a given σ. Specifically, this was done for the maximum and minimum σ expected in geothermal applications. While the functions are not **very** complex, they are not simple enough that an analytical approximation would be superior to a table lookup method.

The program used here initially creates a table of $N(t_D)$ for the given σ, then employs a table lookup/interpolation subroutine for the Hurst function evaluations rather than repeatedly performing the Stehfest inversion. On the Broadlands data, a set of **66** points, a sample execution with repeated Stehfest inversions took over 1100 seconds of CPU time, while the table lookup program took only **45** seconds (on a VAX 11/750). Thus, the radial model is usable even on a microcomputer.

4.3 Field Descriptions

This section contains brief descriptions of the five fields studied in this report. The fields studied cover a full spectrum, ranging from the low-temperature Ellidaar in Iceland to the highly two-phase, high-temperature Broadlands field. The drawdown histories for all the fields are given in the Appendix, their sources are noted in each section below.

4.3.1 Ahuachapan

The Ahuachapan field is located in western El Salvador. The reservoir has areal extent of 7400 acres (Kestin, 1980) with many surface manifestations. The reservoir consists of fractured andesitic rock. The reservoir field temperature is reported as 230 $^\circ C$ by Kestin(1980) and 240 $^\circ C$ by Grant et al.(1982). Initially a fully liquid dominated reservoir, a two-phase zone has formed due to exploitation. Reservoir drawdown history from Marcou (1985).

4.3.2 Broadlands

The Broadlands field is a high temperature geothermal resource located in New Zealand. The reservoir matrix is highly porous but not permeable: flow occurs in fracture zones which exist near faults and formation contacts (Hitchcock and Bixley, 1975). It is a high-temperature (270 °C) liquid dominated reservoir with an extensive two-phase zone (Grant et al., 1982). Reservoir history provided by P. F. Bixley of the Ministry of Works and Development.

4.3.3 Ellidaar

The Ellidaar field is one of three low-temperature fields in Reykjavik. It is a small, low-temperature reservoir. Cooling of up to 10° C has occurred, probably due to cold water influx (Palmasson et al., 1983). Reservoir data from Vatnaskil (1982).

4.3.4 *Svartsengi*

The Svartsengi field is one of three geothermal fields on the Reykjanes Peninsula in southwest Iceland. It is a high-temperature liquid dominated reservoir. High permeability exists throughout the production area. (Gudmundsson and Olsen, 1984). Produced fluids are not currently being reinjected, but the possibility is being studied (Gudmundsson, 1983 and Gudmundsson et al., 1984). Svartsengi drawdown data from Olsen (1984).

4.3.5 Wairakei

The Wairakei, New Zealand, reservoir is approximately 15 km^2 in extent. It is believed that the resource is due to a hot plume rising through cold water from an ultimate magmatic source at depth of 10 km. A two-phase zone exists near the top of the reservoir and has increased with production (Fradkin et al., 1981). Drawdown history for Wairakei from Marcou (1985).

5. RESULTS AND DISCUSSION

Hurst method history matches, both linear and radial cases, were performed on the drawdown data of the five fields (Ahuachapan, Broadlands, Ellidaar, Svartsengi, and Wairakei). The input parameters used in the analyses are given in Table 1. The drawdown data (time, production rate, and drawdown) are given in the Appendix. Graphs of the rate histories are shown in Figures 7-11. (Drawdown histories are shown with the model fits.) Sample plots of standard deviation vs σ and A used for determining the best match for each field are shown in figures 12-21.

The σ, X, a_{lin}, a_{rad}, and standard deviations of the matches on the each field are given in Table 2. The reservoir cornpressibilities and permeability-thickness products resulting from the radial fit are given in Table 3. Plots of actual and modeled drawdown for all fields are given in Figures 22-29.

The linear and radial fits are compared in table 2. Generally, the radial model gave better results (smaller standard deviations). Specifically, the Ahuachapan, Svartsengi, and Wairakei data were best fit by the radial model. For Wairakei, the linear model could not be fit to the entire data history, but could be fit to the early data. Such behavior confirms that it is a strongly radial system (recall discussion, section 4.1). Figures 12, 14, and 16 are the radial fits for those fields, all are reasonable matches that model well the true drawdown behavior of the reservoirs.

In the Broadlands case, the linear model yielded a slightly better fit than did the radial, but from Figs. 24 and 25 it is seen that neither match well. The high compressibility of the Broadlands field explains the poor drawdown predictions of Figures 24 and 25. In those figures, the actual data shows strong variations while the prediction is very stable and insensitive, as if it had a strong pressure support. In a highly compressible fluid, pressure disturbances travel slowly. In the Broadlands field, the delay across the field may be of the order of months (Grant, 1977) What this means is that the aquifer does not feel the pressure drops immediately and so cannot provide the support that the Hurst model thinks it will. Thus, the Hurst model assumes pressure support that is not there. It is encouraging that although the match itself may not be satisfactory, the model yields a reasonable compressibility value: one of the order of the compressibility of two-phase mixture.

The Ellidaar case was handled slightly differently. Figures 20 and 21 show no minimum standard deviation, only a flattening at high σ. This behavior indicates that the line source limit of the Hurst Model should be used. **As** described in Section 3.1.2, the line source's physical interpretation is that the reservoir is small compared to the aquifer, so that the reservoir response is negligible compared to the aquifer response. Thus in the line source limit, reservoir properties cannot be deduced. However, a model fit can still be done. The fit is shown in Fig. 26.

Table **3** gives the compressibilities and thicknesses calculated from the radial matches. The cornpressibilities range from 12.0×10^{-6} for the Broadlands field to 2.8×10^{-8} for Wairakei. From the previous discussion of compressibilities, these lie approximately in the range of values of compressibility of water systems in the configurations discussed. This confirms that the Broadlands field is highly two-phase while at the other extreme Wairakei is mainly liquid with little two-phase zone.

It was stated earlier that reservoir compressibility is an important quantity to determine from a history match. (Its wide range of possible values means it can not be easily estimated initially, but once determined, it gives an estimate of the extent of the two-phase zone.) It was also seen that the radial model accomplishes this end most easily, as compressibility is calculated from σ with less dependence on the geometric term (which is often uncertain). Table **3** shows that the radial model is generally applicable, and yielded reasonable compressibility results. The Hurst radial model is thus applicable to a large range of reservoirs and easy to use with little reservoir information. It yields reasonable values for reservoir parameters, and history matches with predictive capability.

6. CONCLUSIONS

1. Reservoir compressibility is an important parameter to determine for a field for two reasons: compressibility has such a large range of values that it is not readily estimable initially, and its value is useful as a way of estimating the extent or existence of a two-phase zone in a liquid dominated geothermal reservoir.

2. The Hurst Simplified Method history match yields useful reservoir parameters (c and kh) as well as a model useful in prediction.

3. The matches on the various fields showed that the Hurst radial model is useful on a wide range of liquid-dominated geothermal reservoirs.

4. Comparing the standard deviation of the best linear and radial matches tells whether the reservoir geometry is closer to linear or radial.

5. In highly compressible (highly two-,phase) systems, the Hurst model yields a reasonable compressibility, but the match itself has difficulty modeling the sharp changes in drawdown well.

6. A flattening of the σ vs standard deviation curve at high σ (rather than a true minimum) indicates that the field is small, and that the line source limit of the Hurst Model should be used. In that case, a match (and predictions) can still be done, but reservoir characteristics cannot be determined.

7. Using a table-lookup formulation of the Hurst radial model, execution time was cut drastically, enough that the radial history match could be carried out on a microcomputer.

NOMENCLATURE

A	Area of the reservoir or cross-sectional area of the aquifer (m^2)
B	Van Everdingen and Hurst water influx constant (kg/Pa)
C	Heat capacity (kJ/kg·°K)
c	Compressibility (Pa^{-1})
g	Acceleration of gravity (9.81 m/s^2)
h	Height of reservoir (m)
k	Permeability (m^2)
l	Length of reservoir (m)
L	Length of aquifer (m)
M,N	Hurst functions
P	Pressure (Pa)
Q	Hurst influx function
r	Radius (m)
s	Variable in Laplace space
S	Saturation
t	Time (s)
T	Temperature (K)
V	Volume (m^3)
w	Mass rate (kg/s)
W	Mass (kg)
x,y	Least squares variable
μ	Viscosity (Pa s)

φ	Porosity
ρ	Density (kg/m^3)
λ, σ	Hurst parameters

SUBSCRIPTS

a	Aquifer
av	Average
D	Dimensionless
e	Encroached
f	Formation
i	Initial
m	Matrix
p	Produced
r	Reservoir
s	Steam
sat	Saturated conditions
T	Total or isothermal
w	Liquid water

Barred variables indicate Laplace space form.

REFERENCES

Allard, D. R., and Chen, S. M.: "Calculation of Water Influx for Bottom-Water Drive Reservoirs", Soc. Pet. Eng. Tech. Paper 13170 (1984).

Atkinson, P., Celati, R., Corsi, R., Kucuk, F. and Ramey, H. J. Jr.: "Thermodynamic Behavior of the Bagnore Geothermal Field", Geothermics (1978) Vol. 7, 185-208.

Bolton, R. S.,: The behavior of the Wairakei geothermal field during exploitation", U.N. Geothermal Symposium, Vol. 2, 1426-1439.

Brigham, W. E., and Morrow, W. B.: "p/Z Behavior for Geothermal Steam Reservoirs", Soc. Pet. Eng. J. (December 1977).

Brigham, W. E., and Neri, G.: "Preliminary results on a depletion model for the Gabbro zone", Fifth Stanford U. Geothermal Workshop (1979).

Carter, R. D. and Tracy, C. W.: "An improved method for calculating water influx", Trans. AIME (1960), Vol 216, 415-17.

Craft, B. C.. and Hawkins, M. F.: Applied Petroleum Reservoir Engineering, Prentice-Hall, New Jersey (1959).

Donaldson, I. G., Grant, M. A., and Bixley, P. F.:"Nonstatic Reservoirs: The Natural State of the Geothermal Reservoir", J. Pet. Tech. (January, 1983), 189-194.

Earlougher. R. C. Jr.: Advances in Well Test Analysis, Soc. Pet. Eng., New York (1977).

Fetkovitch, M. J.: "A Simplified Approach to Water Influx Calculations -- Finite Aquifer Systems", J. Pet. Tech., (July, 1971).

Fradkin, L. J., Sorey, M. L., and McNabb, A.: "On Identification and Validation of Some Geothermal Models", Water Resources Research, (August, 1981), 929-936.

Grant, M. A.: "Broadlands -- A gas-dominated geothermal field", Geothermics, (1977), Vol. 6, 9-29

Grant, M. A.: "Effect of Cold Water Entry Into a Liquid-Dominated Two-Phase Geothermal Reservoir", Water Resources Research, (August, 1981), 1033-43.

Grant, M. A.: "Geothermal Reservoir Modeling", Geothermics (1983), Vol 12, 251-263.

Grant, M. A. and Sorey, M. L.: "The Compressibility and Hydraulic Diffusivity of a Water-Steam Flow", Water Resources Research, (June, 1979), Vol. 15, 684-6.

Grant, M. A., Donaldson, I. G., and Bixley, P. F.: Geothermal Reservoir Engineering, Academic Press, New York (1982).

Gudmundsson, J. S.: "Injection Testing in 1982 at the Svartsengi High-Temperature Field in Iceland", Trans. Geothermal Resources Council (October 1983), 423-8.

Gudmundsson, J. S.: "Composite Model of Geothermal Reservoirs", Bulletin, Geothermal Resources Council, (January 1986), 3-10.

Gudmundsson, J. S. and Olsen, G.: "Water Influx Modeling of Svartsengi Geothermal Field, Iceland", Soc. Pet. Eng. Tech. Paper 13615, (1985).

Gudmundsson, J. S., Hauksson, T., Thorallsson, S., Albertsson, A., and Thorolfsson, G.: "Injection and Tracer Testing in Svartsengi Field, Iceland", 6th New Zealand Geothermal Workshop, (November, 1984).

Hitchcock, G. W., and Bixley, P. F.: "Observations of the Effect of a Three-Year Shutdown at Broadlands Geothermal Field, New Zealand", Second U. N. Geothermal Workshop, (1976), 1657-61.

Hurst, W.: "The Simplification of the Material Balance Formulas by the Laplace Transformation", Trans. AIME (1953), 292-304.

Kestin, J., DiPippo, R., Khalifa, H. E., and Ryley, D. J., eds.: Sourcebook on the Production of Electricity from Geothermal Energy, U. S. Gov't Printing Office, Washington, D. C. (1980).

Macias-Chapa, L.: "Multiphase, Multicomponent Compressibility in Petroleum Reservoir Engineering", Stanford Geothermal Program report SGP-TR-88, (1985).

Marcou, J.: "Optimizing Development Strategy for Liquid Dominated Geothermal Reservoirs", Engineer's thesis, Stanford University, (July 1985).

Martin, J. C.: "Analysis of Internal Steam Drive in Geothermal Reservoirs", J. Pet. Tech., (December 1975), 1493-9.

McNabb, A.: "A Model of the Wairakei Geothermal Field", Appl. Math. Div., Dept. Sci. Ind. Res. (unpublished report, 1975).

Olsen, G.: "Depletion Modeling of Liquid Dominated Geothermal Reservoirs", Master's Report, Stanford University (June, 1984).

Palmasson, G., Stefansson, V., Thorallsson, S. and Thorsteinsson, T.: "Geothermal Field Developments in Iceland", Proceedings, Stanford U. Geothermal Workshop (Dec 1983), 37-51.

Ramey, H. J. Jr.: "Rapid Method of Estimating Reservoir Compressibility", J. Pet. Tech., (April, 1964), 447-454.

Regaldo J. R.: "A Study of the Response to Exploitation of the Svartsengi Geothermal Field, SW Iceland", Report 1981-7, UNU Geothermal Training Program, Reykjavik, Iceland (1981).

Schilthuis, R. J.: "Active Oil and Reservoir Energy", Trans. AIME (1936). 118-31.

Stehfest, H.: "Algorithm 368, Numerical Inversion of Laplace Transforms", D-5 Communications of the ACM (Jan. 1970), 13, No. 1, 47-9.

van Everdingen, A. F. and Hurst, W.: "The Application of the Laplace Transformation to Flow Problems in Reservoirs", Trans. AIME (Dec. 1949), 305-324.

Vatnaskil: "Gagnaskra fyrir vinnslugolur" (private report in Icelandic) (1982).

Whiting, R. L., and Ramey, H. J. Jr.: "Application of Material and Energy Balances to Geothermal Steam Production", J. Pet. Tech., (July, 1969), 893-900.

	PERMEABILITY $k\ (\times 10^{-12}\ m^2)$	POROSITY φ	AREA $A\ (x\,10^6\ m^2)$	TEMPERATURE $T\ (^\circ C)$
Ahuachapan	.050	.21	15.0	240.
Broadlands	.829	.15	2.0	270.
Ellidaar	.099	.05	1.0	110.
Svartsengi	.500	.05	3.6	240.
Wairakei	.027	.20	15.0	260.

TABLE-1. Reservoir parameters input to the history matches.

	LINEAR			RADIAL		
	λ $\times 10^{-5}$	a_{lin} $\times 10^{-10}$	STD. DEV.	σ $\times 10^{-4}$	a_{rad}	STD. DEV.
Ahuachapan	12.1	15.8	5.82	373.	.133	5.69
Broadlands	0.91	0.13	1.16	1.6	.040	1.19
Ellidaar	*	*	*	lss	lss	18.6
Svartsengi	11.5	4.31	2.05	16.	.087	1.77
Wairakei	*	*	*	720.	,072	6.56

* -- **No** linear fit
lss – Line source limiting case

TABLE-2. Hurst parameters, least-squares constants and standard deviations **of** best linear and radial fits **for** each field.

	RESERVOIR COMPRESSIBILITY $c_r (\times 10^{-8} Pa^{-1})$	PERM.-THICK. PRODUCT kh (D-m)
Ahuachapan	5.2	17.4
Broadlands	1200.	6.1
Svartsengi	118.	26.3
Wairakei	2.8	33.4

TABLE-3. **Compressibilities and permeability-thickness products found** from the **radial fits.**

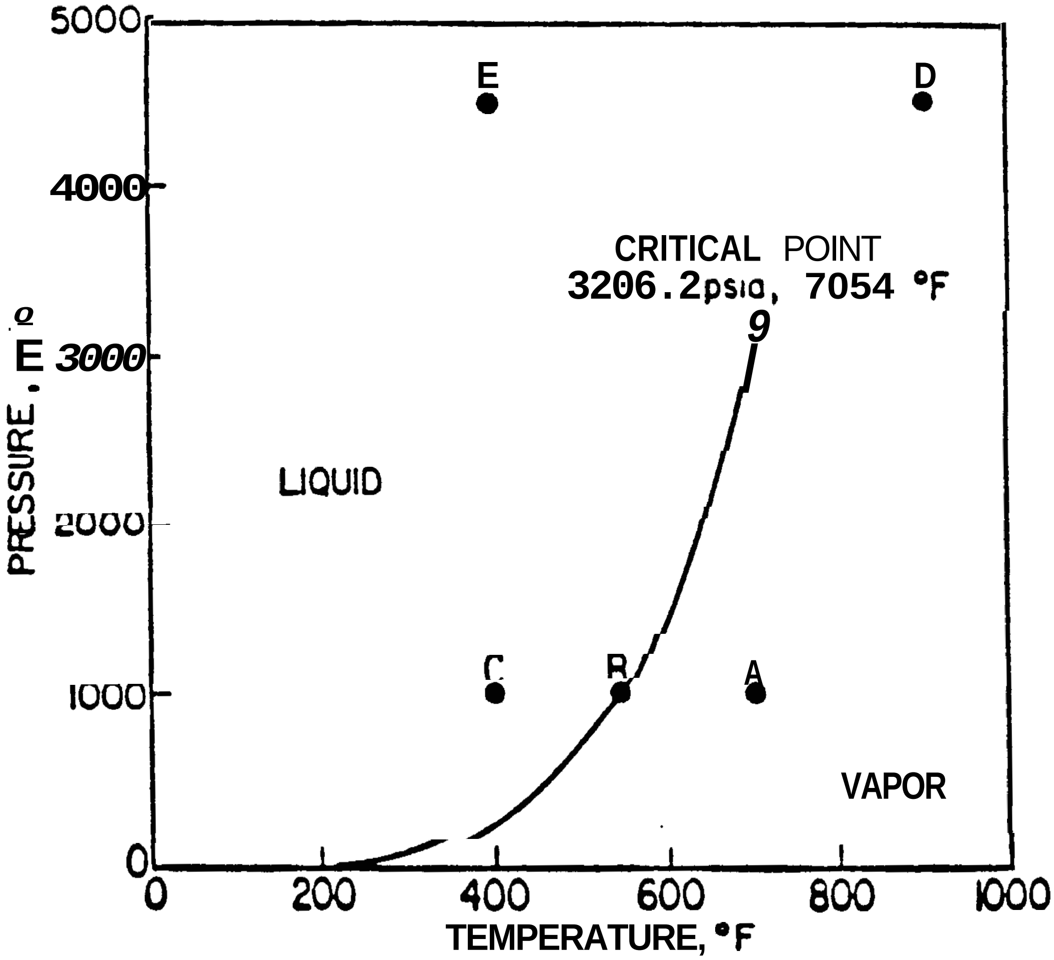

FIGURE-1. **Vapor pressure curve for** pure **water. (Whiting and** Ramey, **1969)**

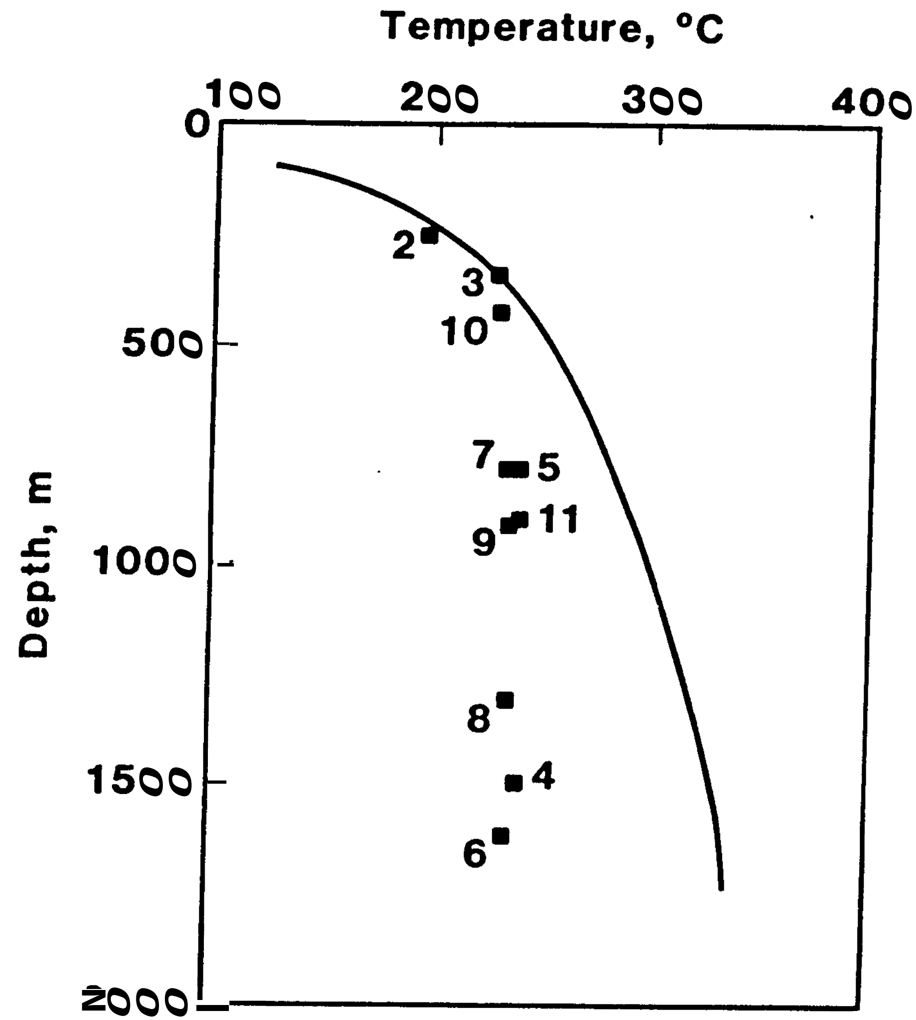

FIGURE-2. Reservoir temperature with depth at Svartsengi (Gudmundsson, 1986)

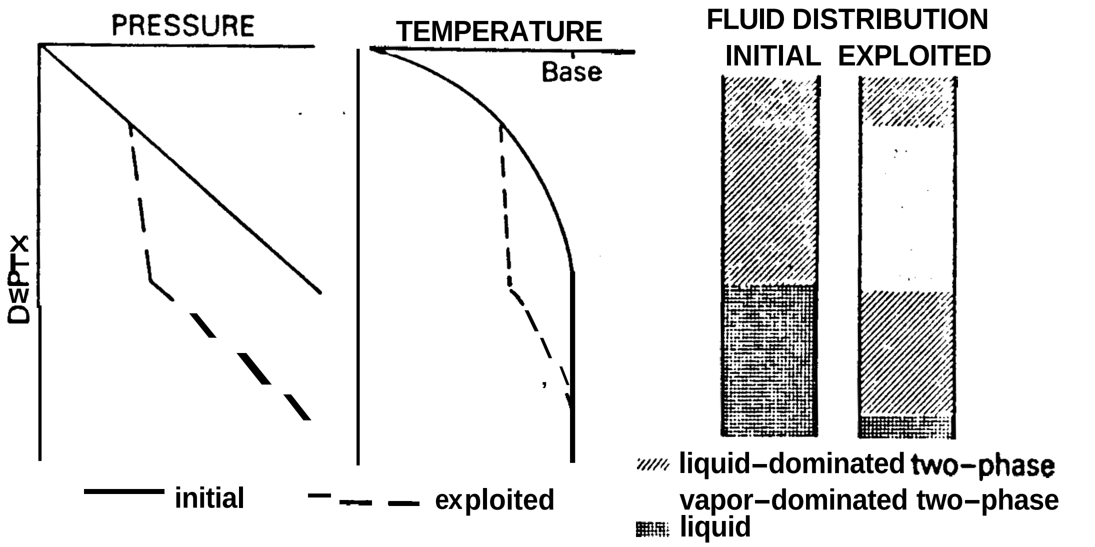

Fig. 2.14. Liquid-dominated reservoir developing a steam cap under exploitation. (After Bolton, 1970, and McNabb, 1975).

FIGURE-3. Liquid dominated reservoir developing a two-phase zone due to exploitation. (Grant, et al., 1982, after Bolton, 1970 and McNabb, 1975)

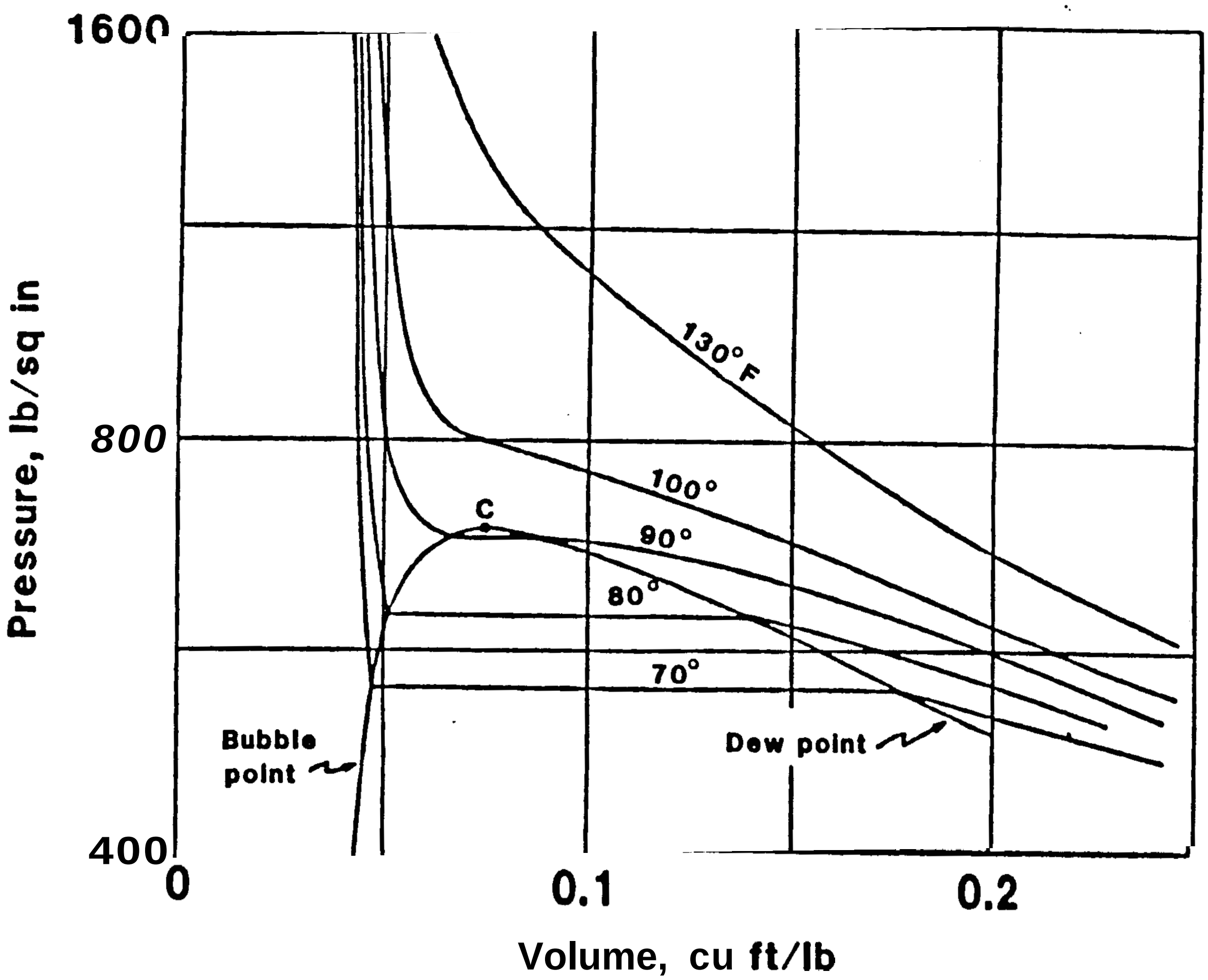

FIGURE-4. Pressure versus specific volume for a pure material. (Macias-Chapa, 1985)

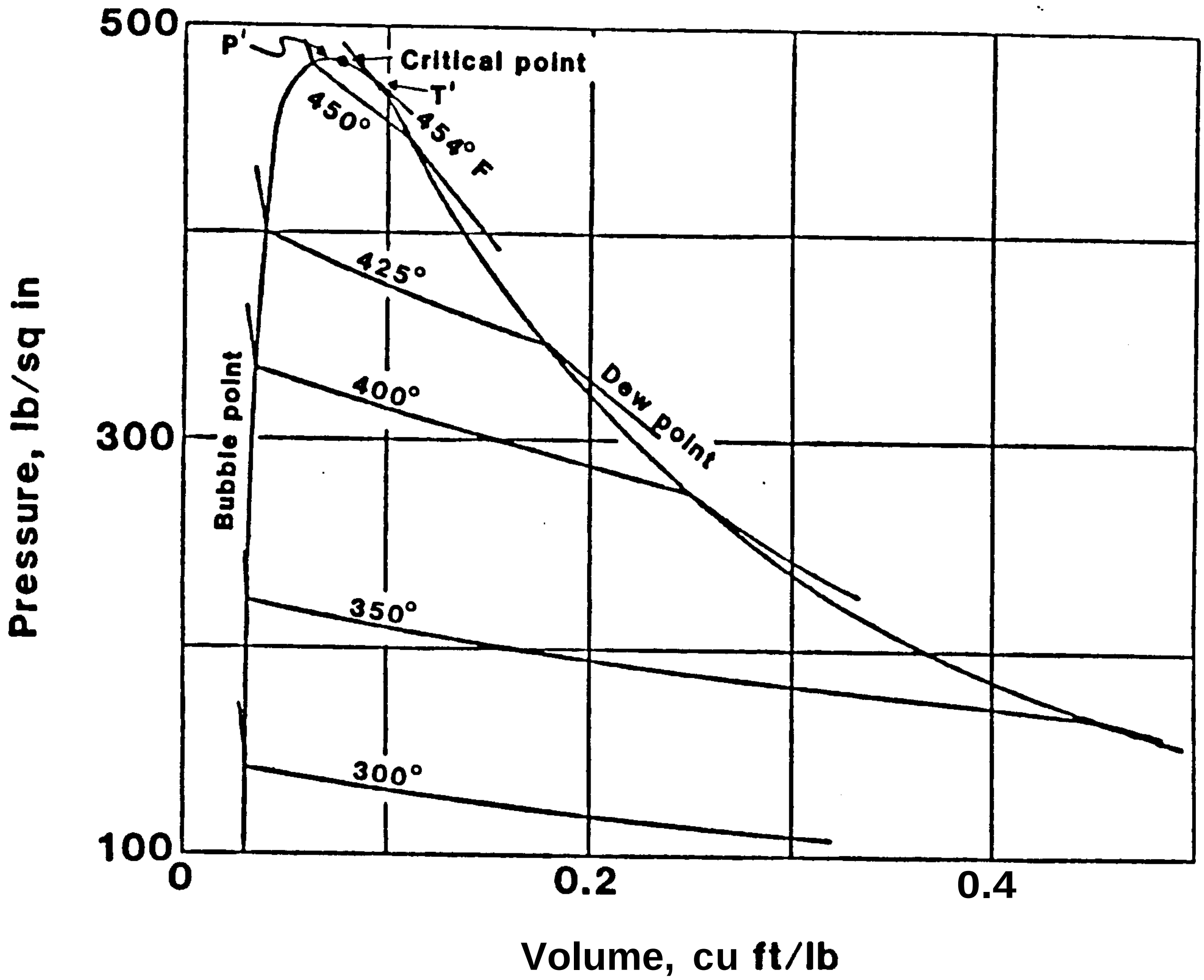

FIGURE-5. **Pressure versus** specific **volume** for **a binary** mixture. (Macias-Chapa, *1985)*

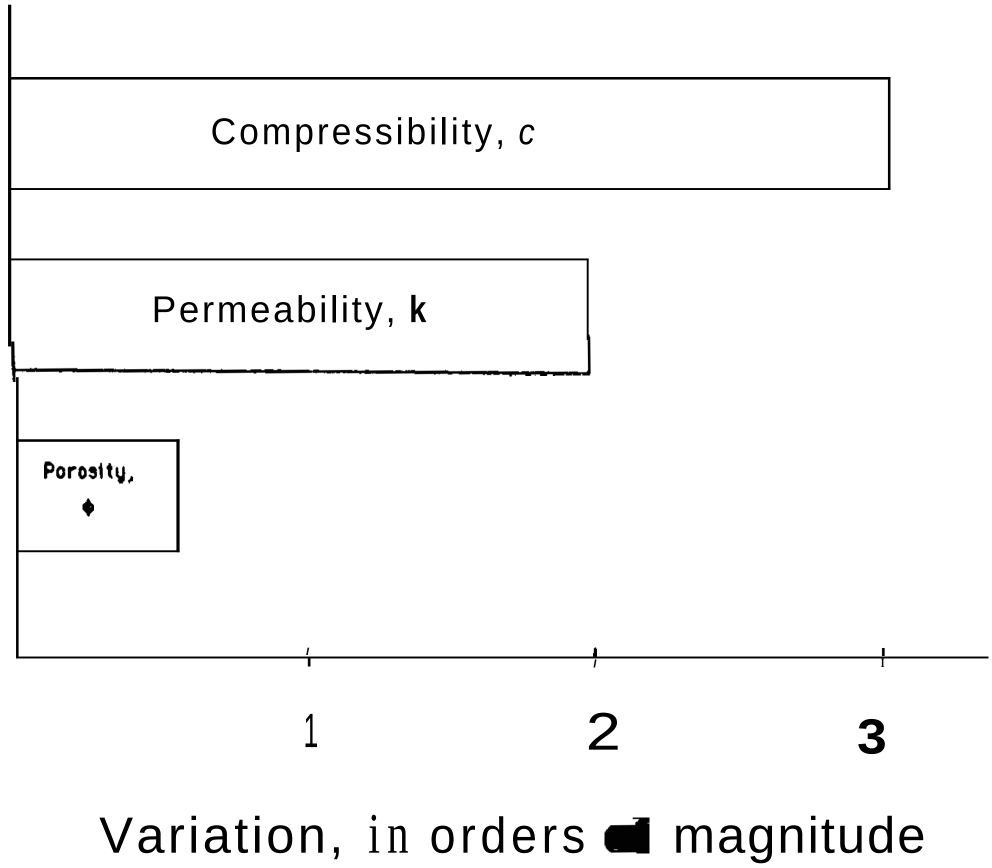

FIGURE-6. Comparison of the variability of model input parameters.

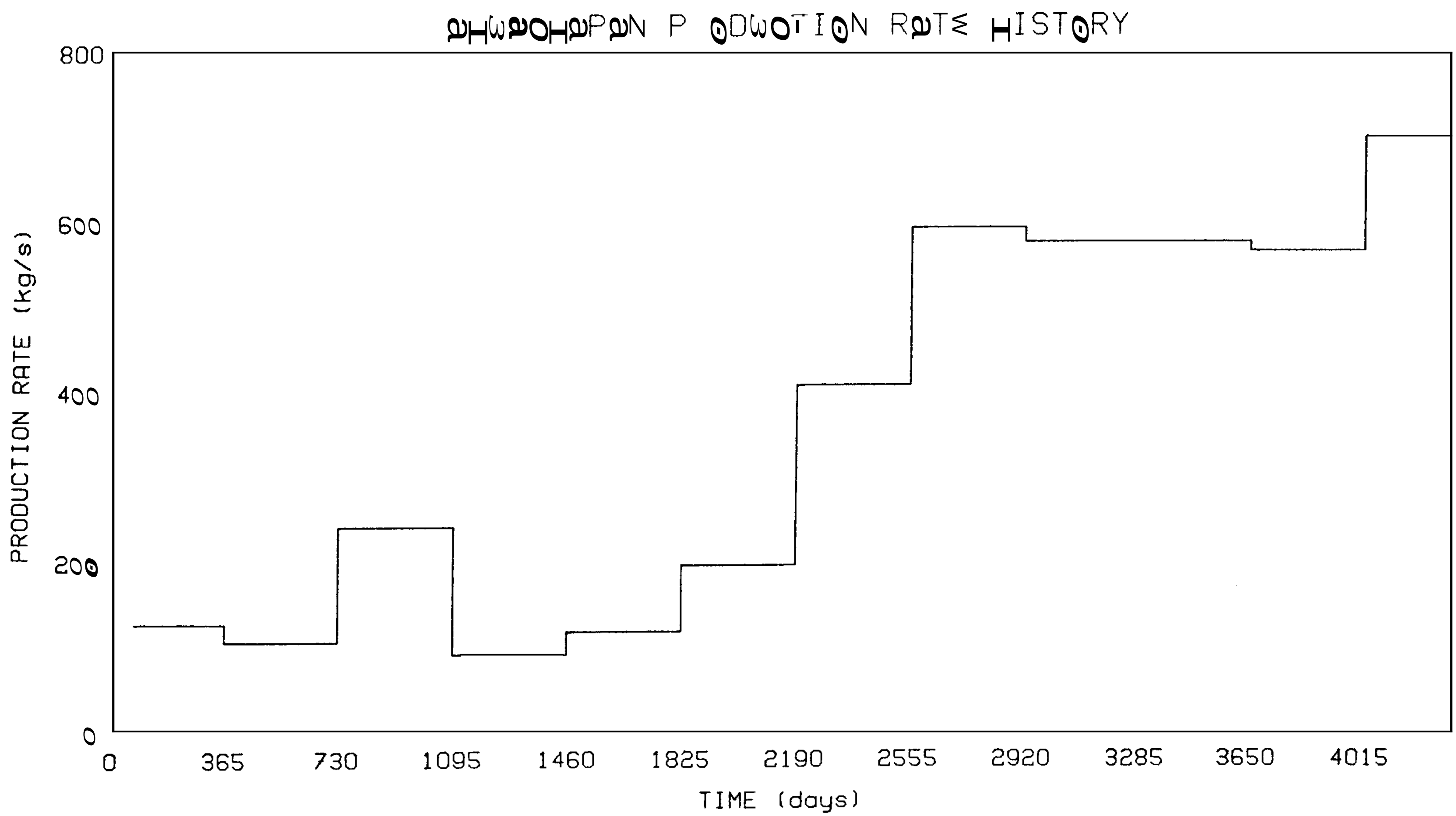

FIGURE-7. Production history of the Ahuachapan field.

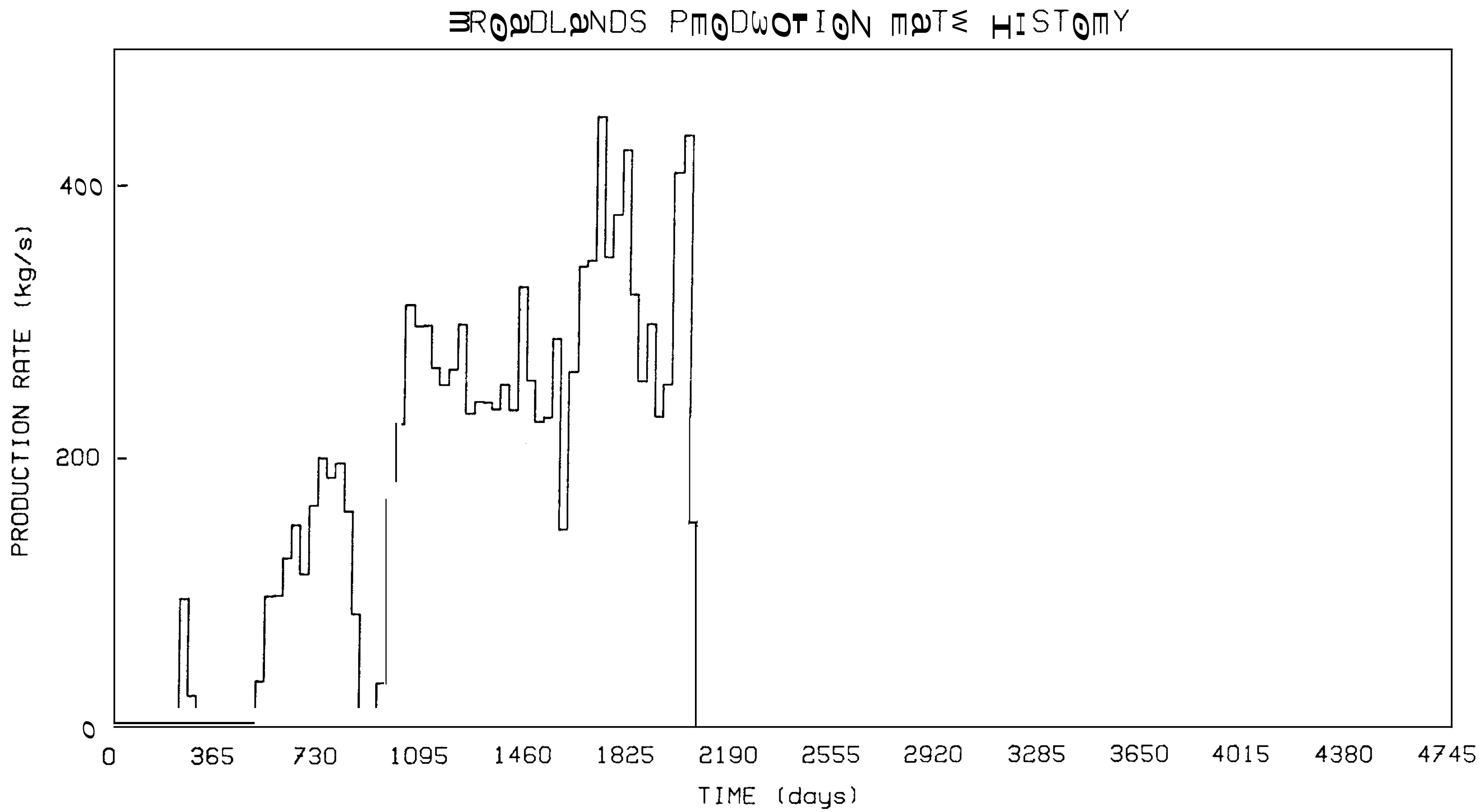

FIGURE-8. Production history of the Broadlands field

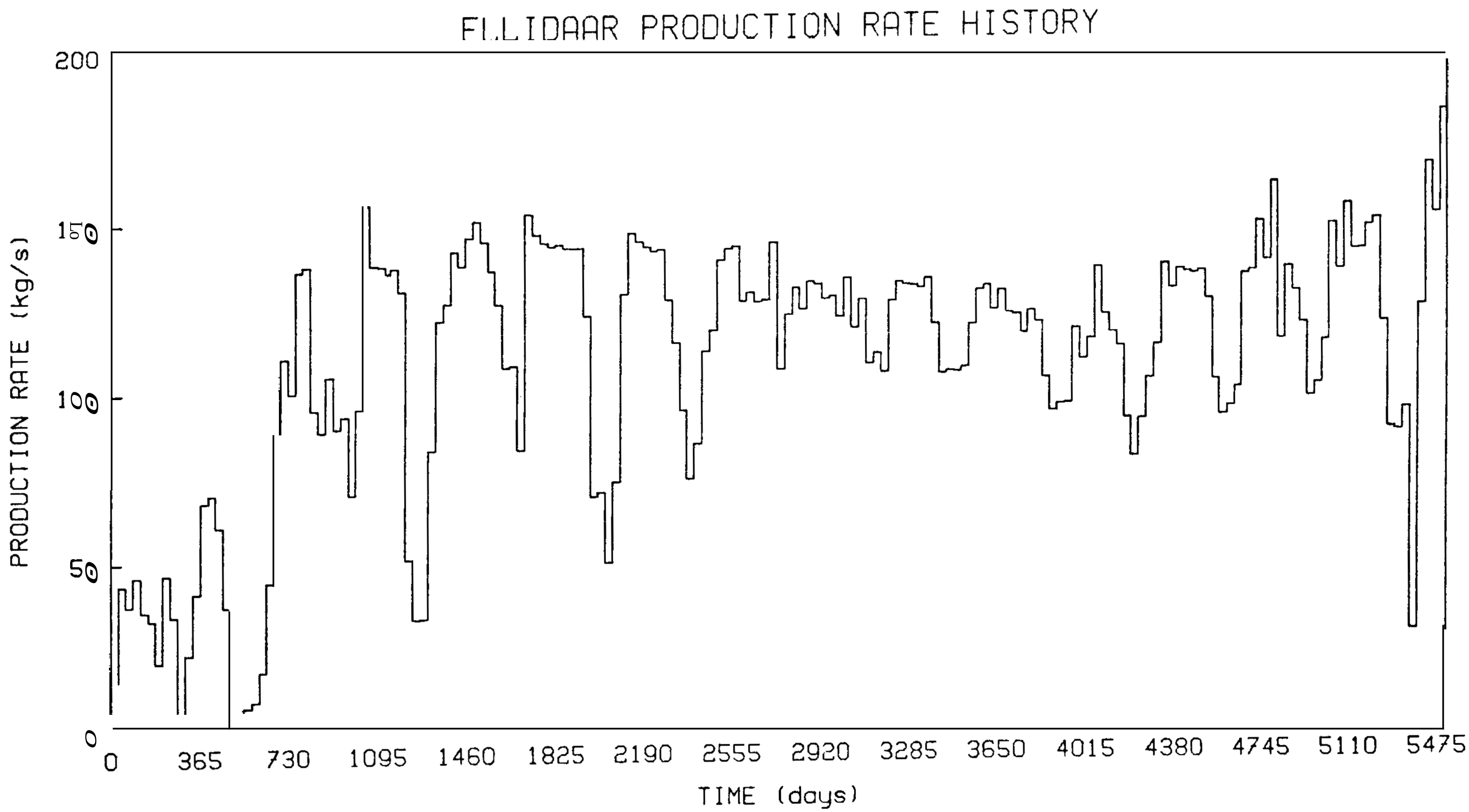

FIGURE-9. Production history of the Ellidaar field.

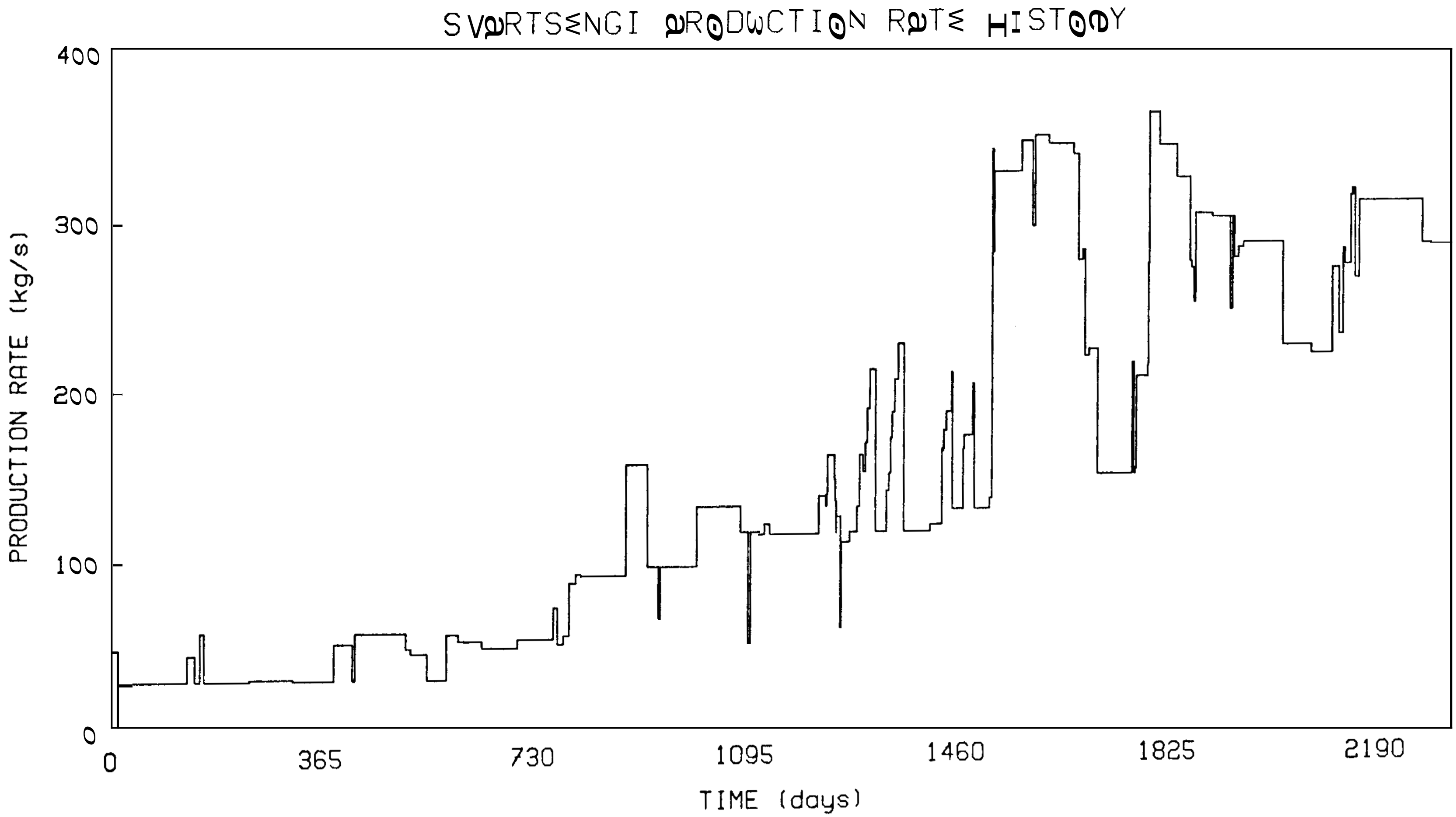

FIGURE-10. Production history of the Svartsengi field.

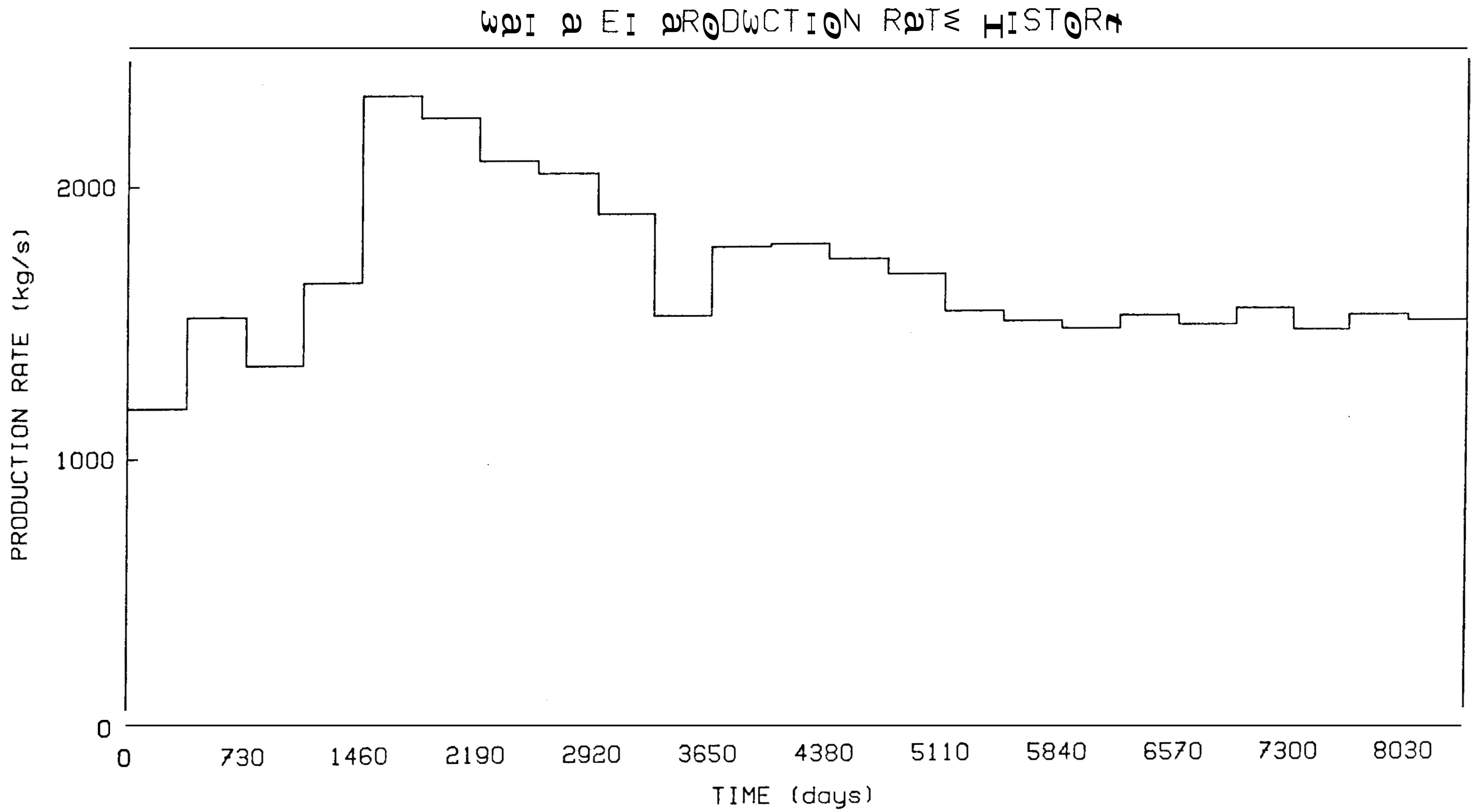

FIGURE-11. Production history of the Wairakei field.

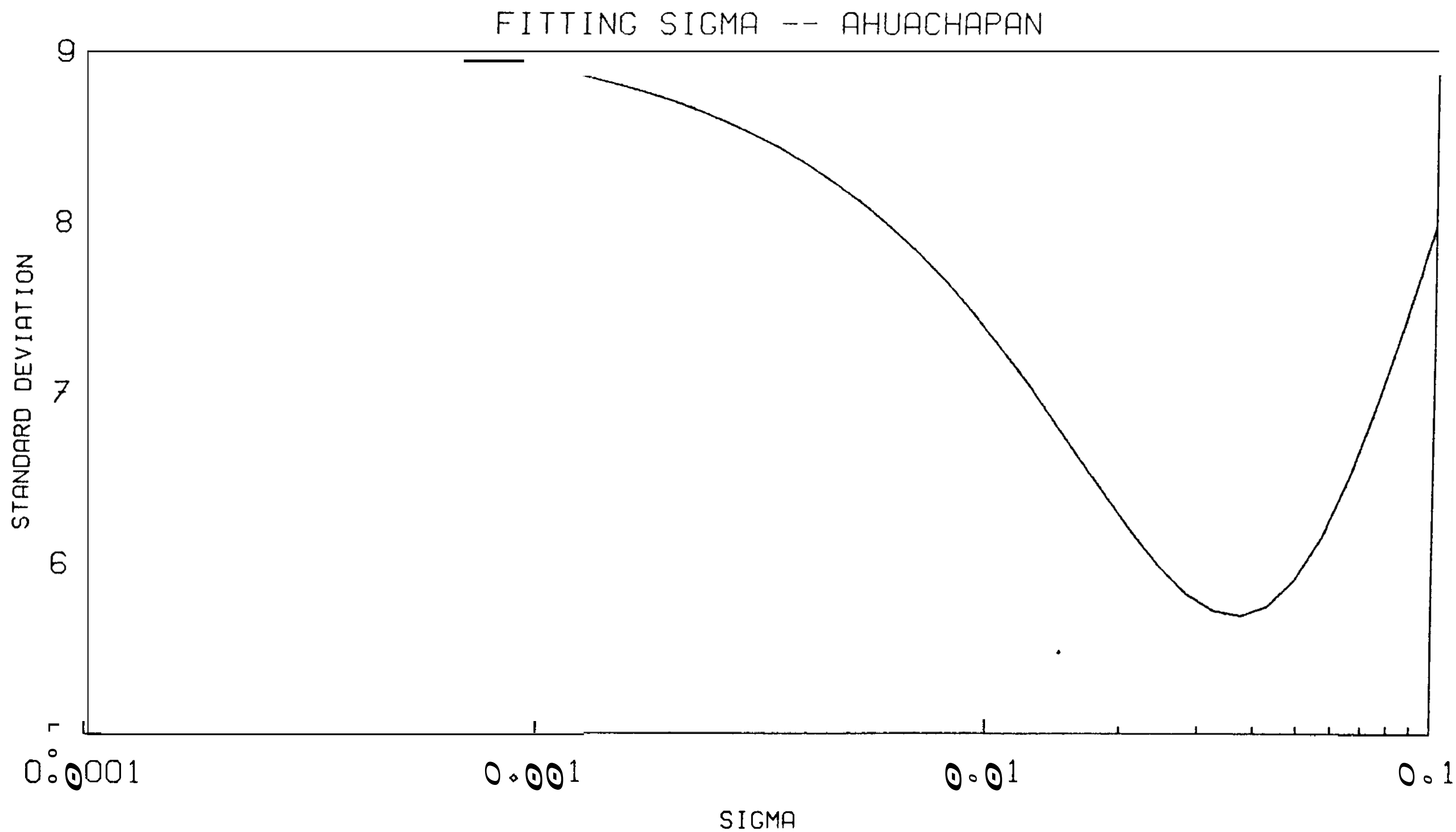

FIGURE-12. Standard deviation vs sigma (radial fit) for Ahuachapan.

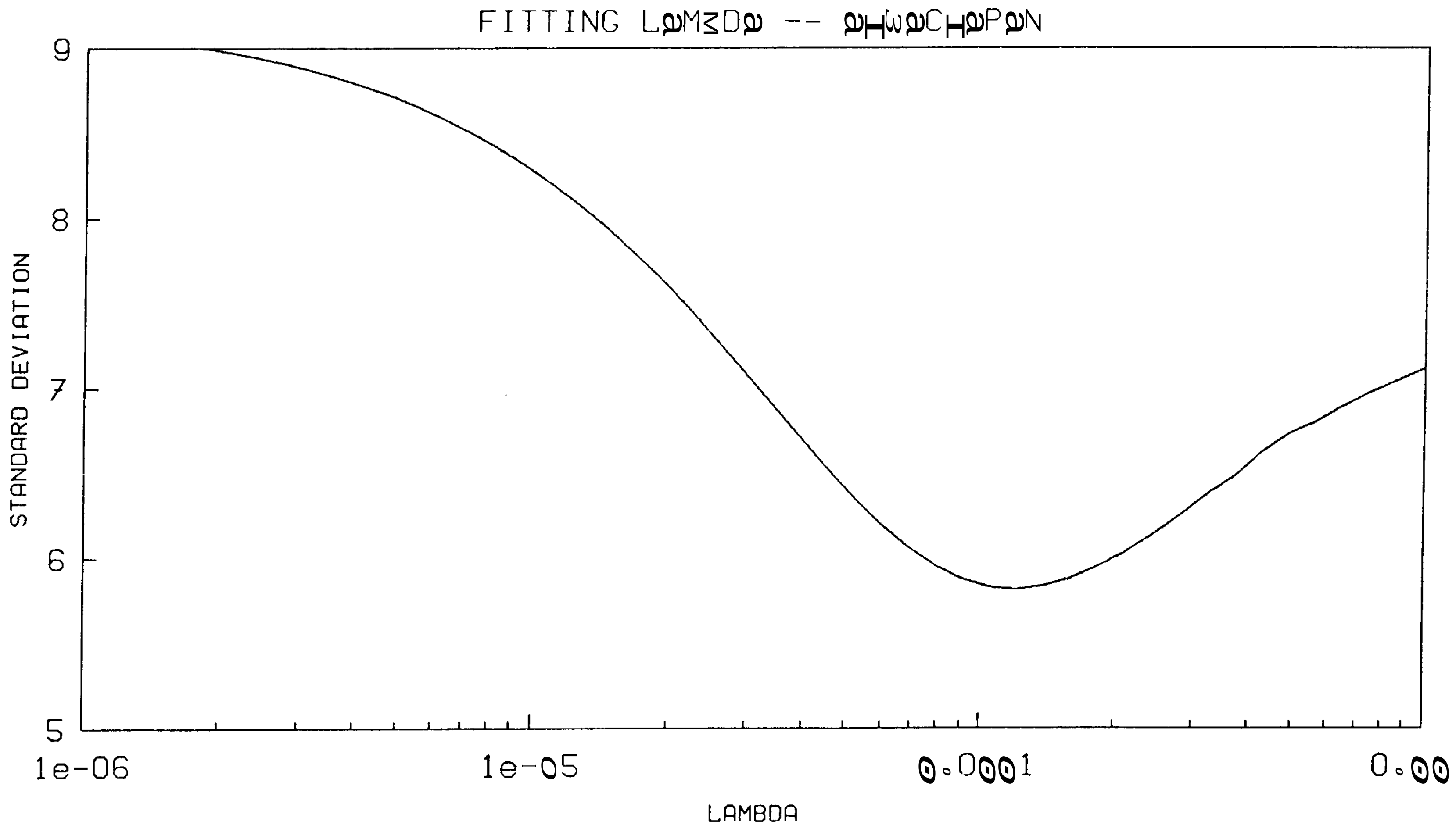

FIGURE-13. Standard deviation vs lambda (linear fit) for Ahuachapan.

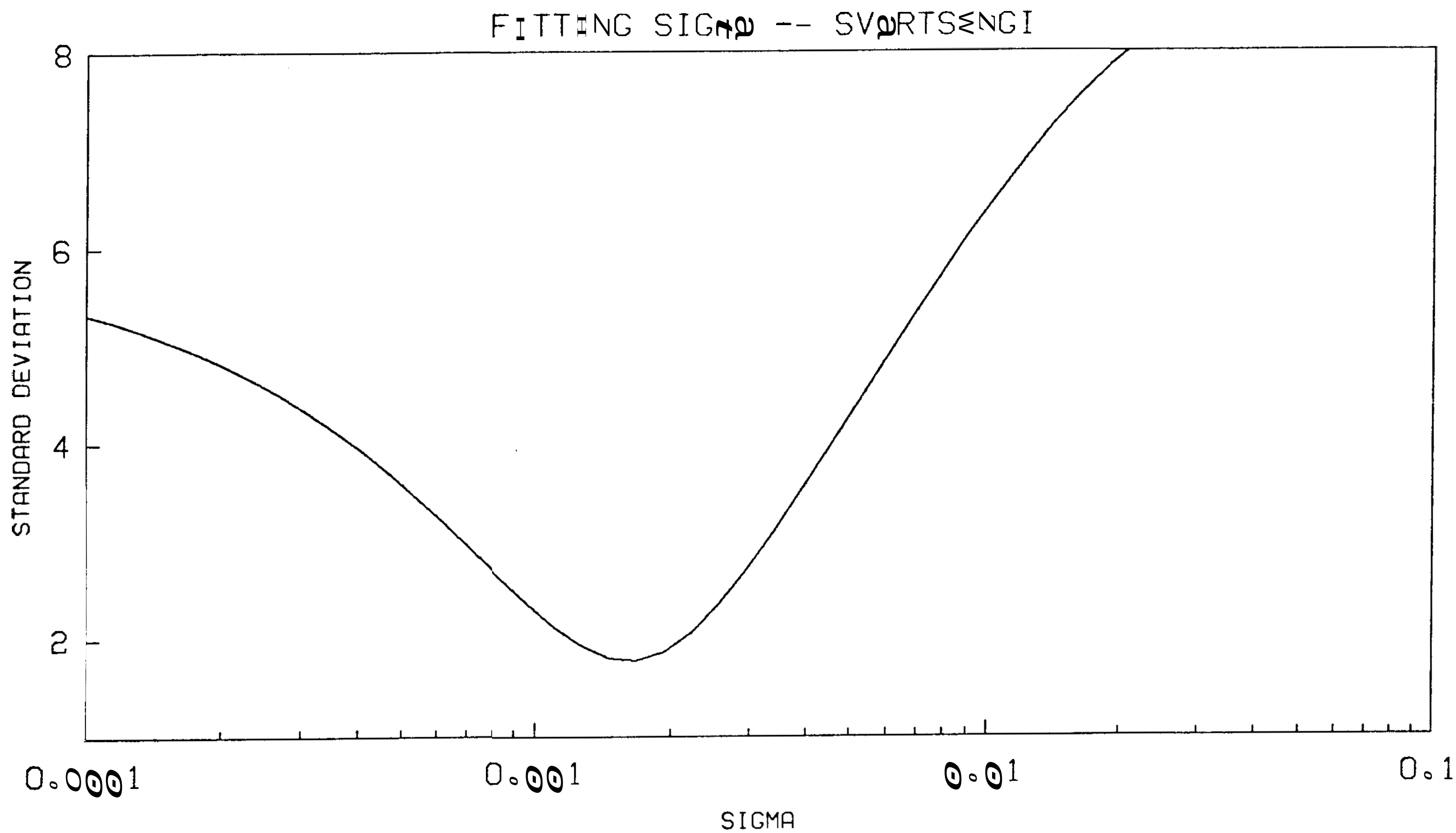

FIGURE-14. Standard deviation vs sigma (radial fit) for Svartsengi

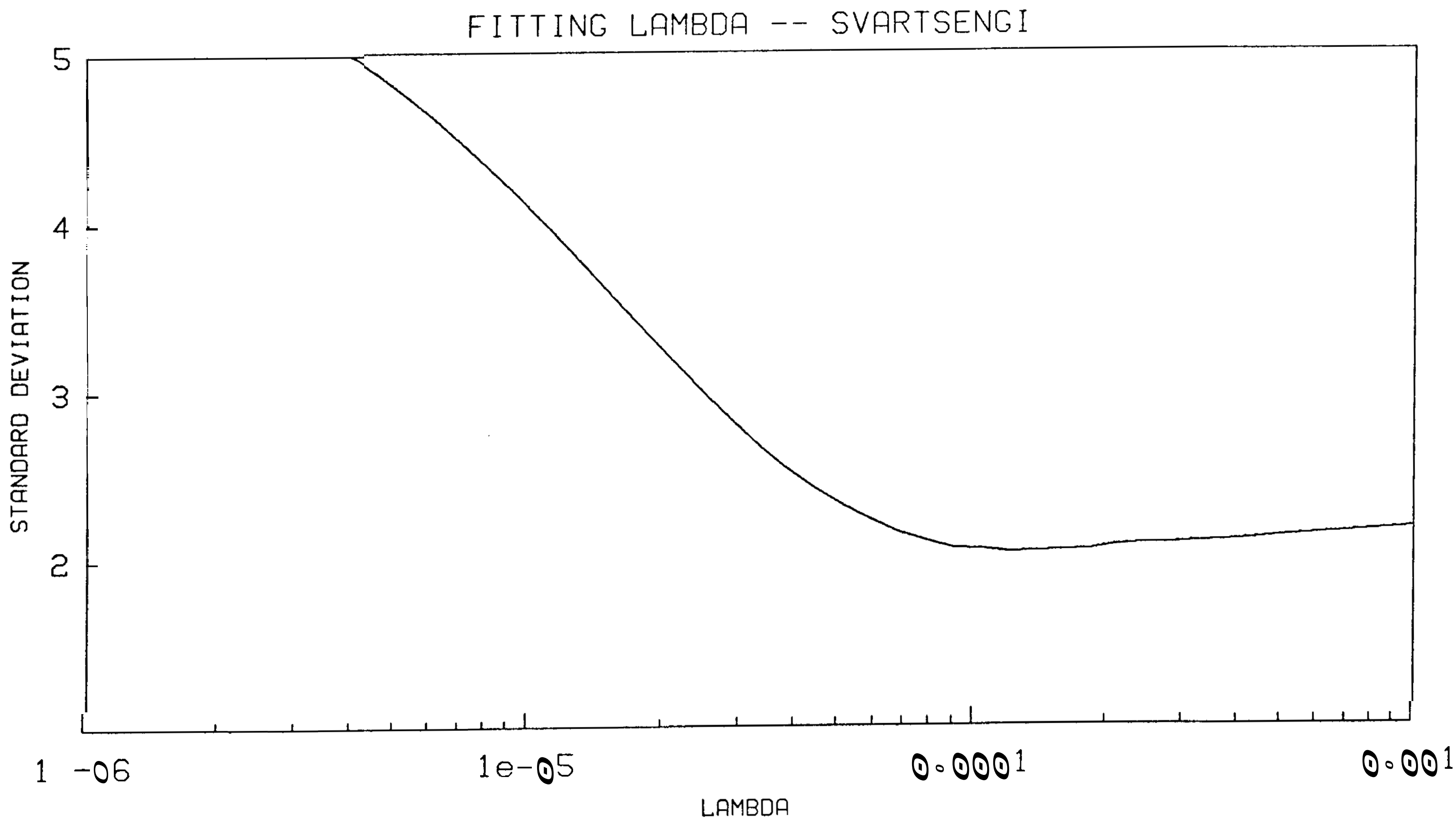

FIGURE-15. Standard deviation lambda (linear fit) for Svartsengi.

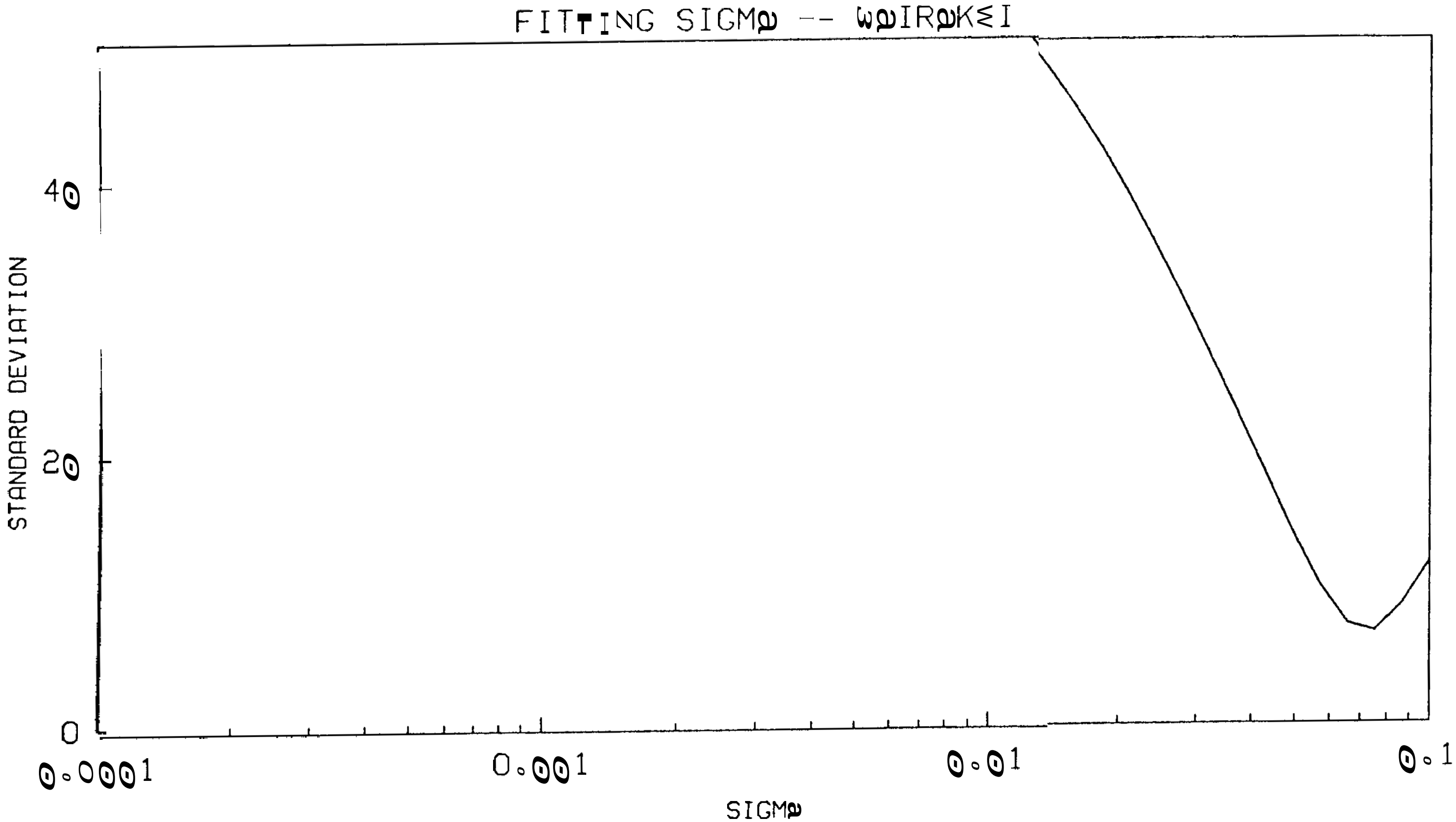

FIGURE-16. Standard deviation vs sigma (radial fit) for Wairakei

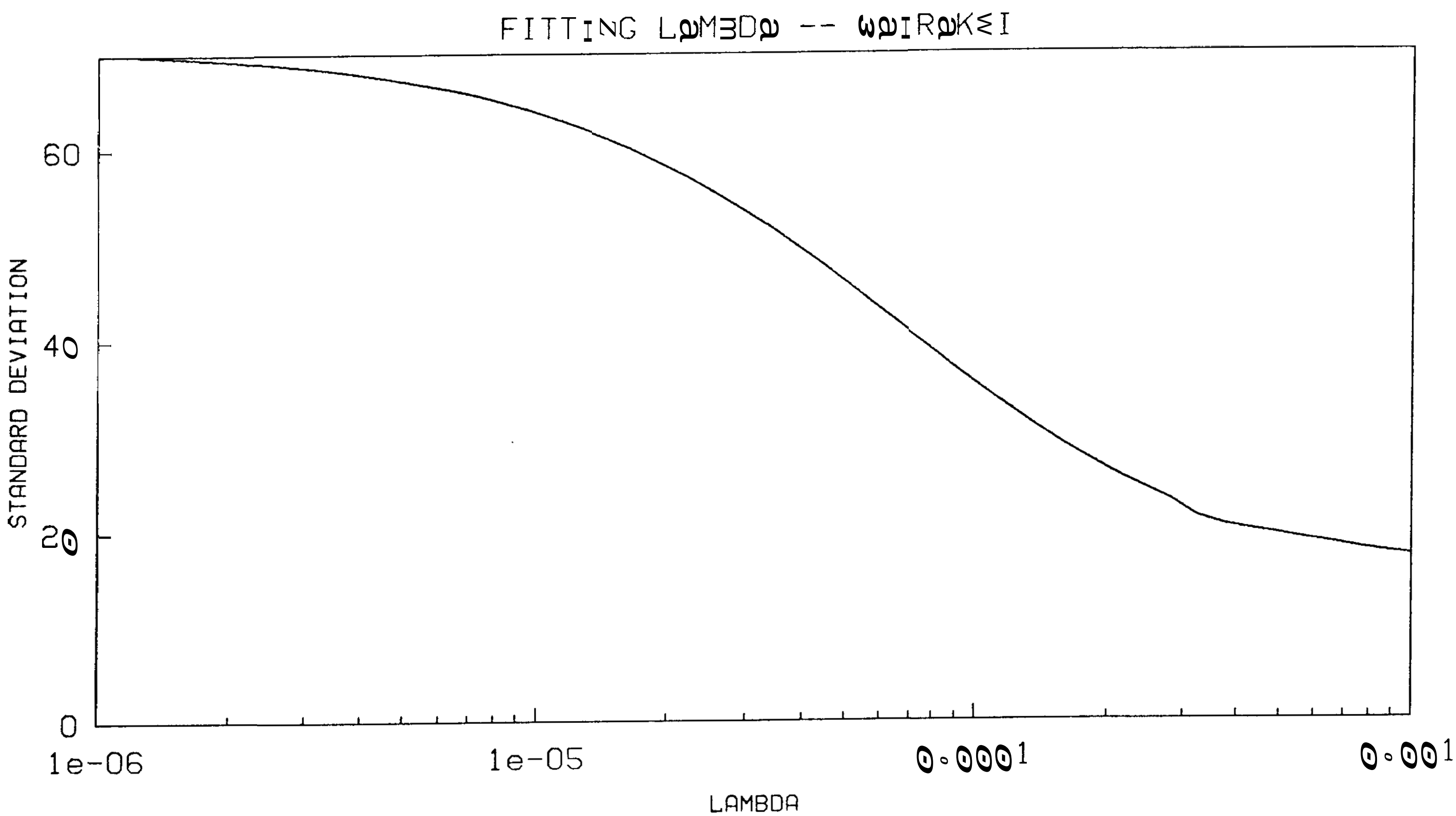

FIGURE-17. Standard deviation vs lambda (linear fit) for Wairakei.

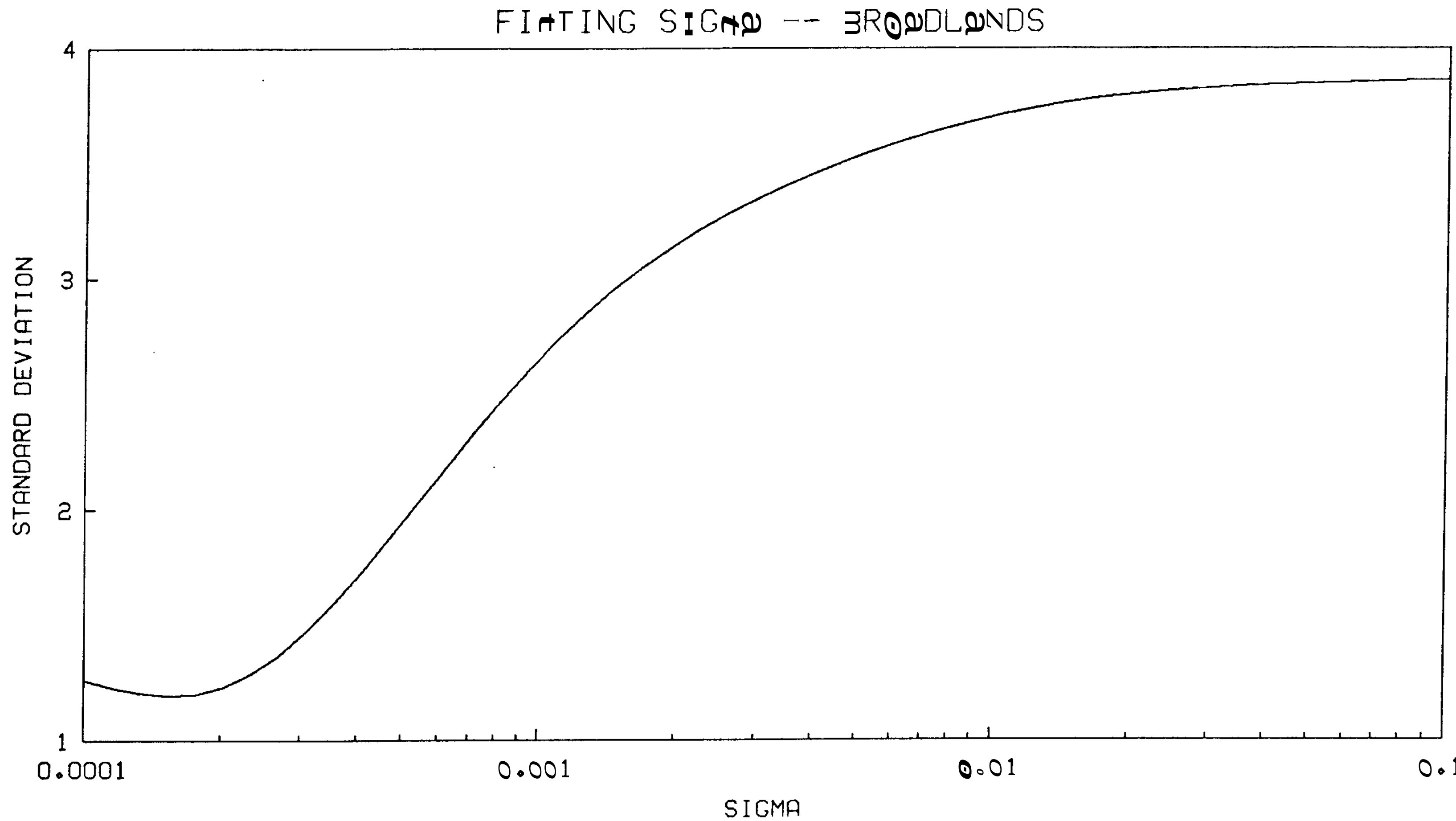

FIGURE-18. Standard deviation vs sigma (radial fit) for Broadlands.

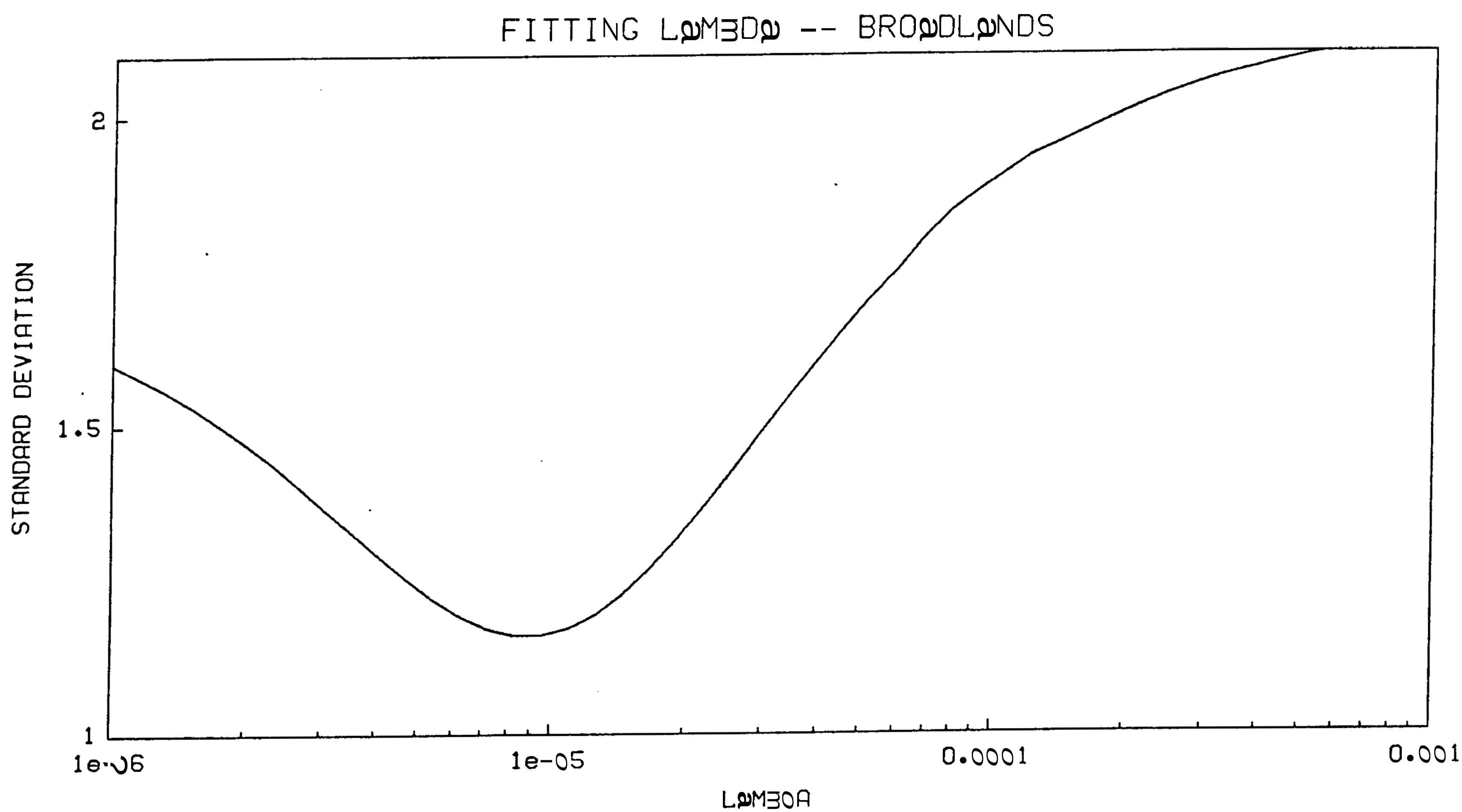

FIGURE-19. Standard deviation vs lambda (linear fit) for Broadlands.

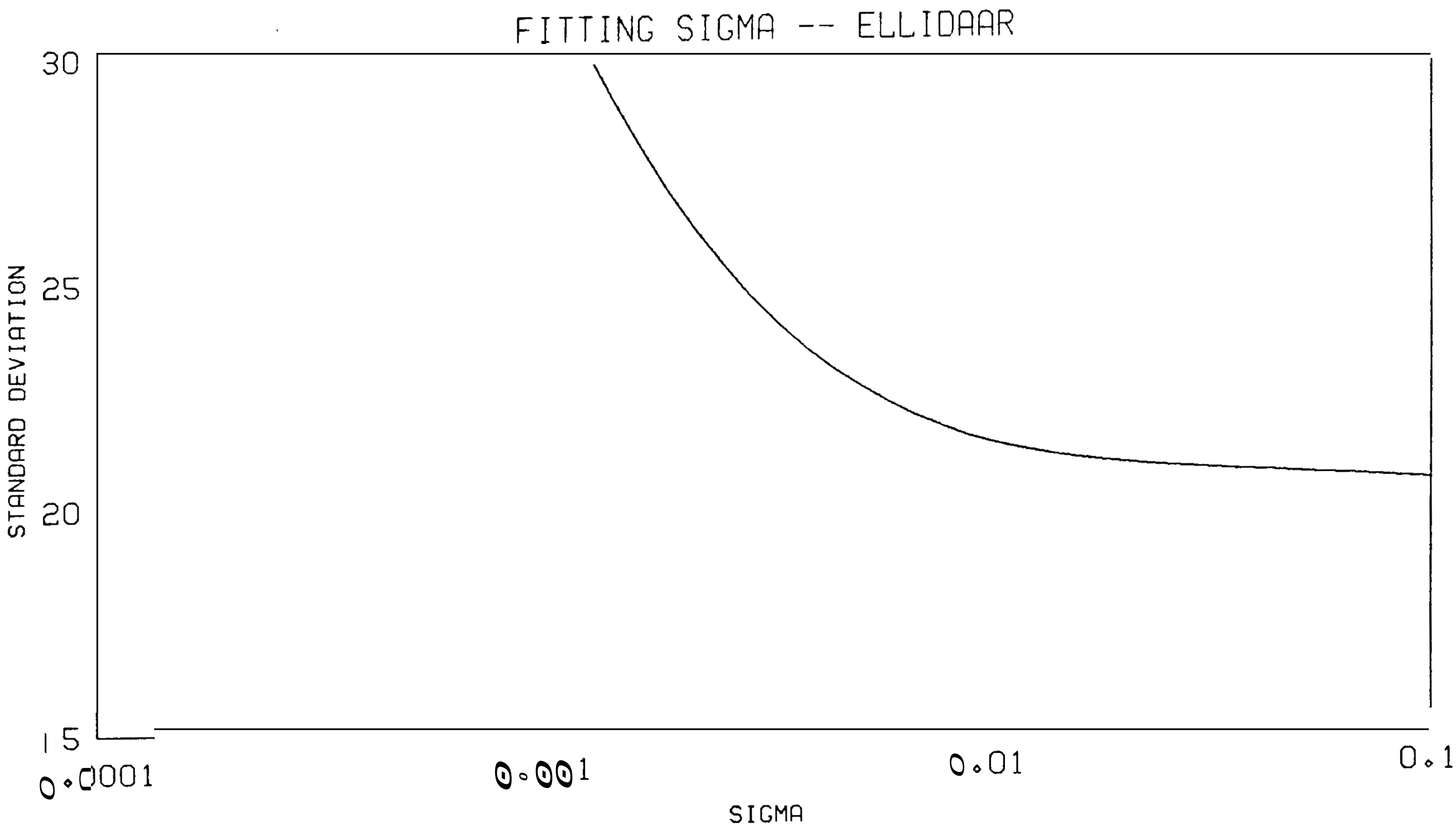

FIGURE-20. Standard deviation vs sigma (radial fit) for Ellidaar.

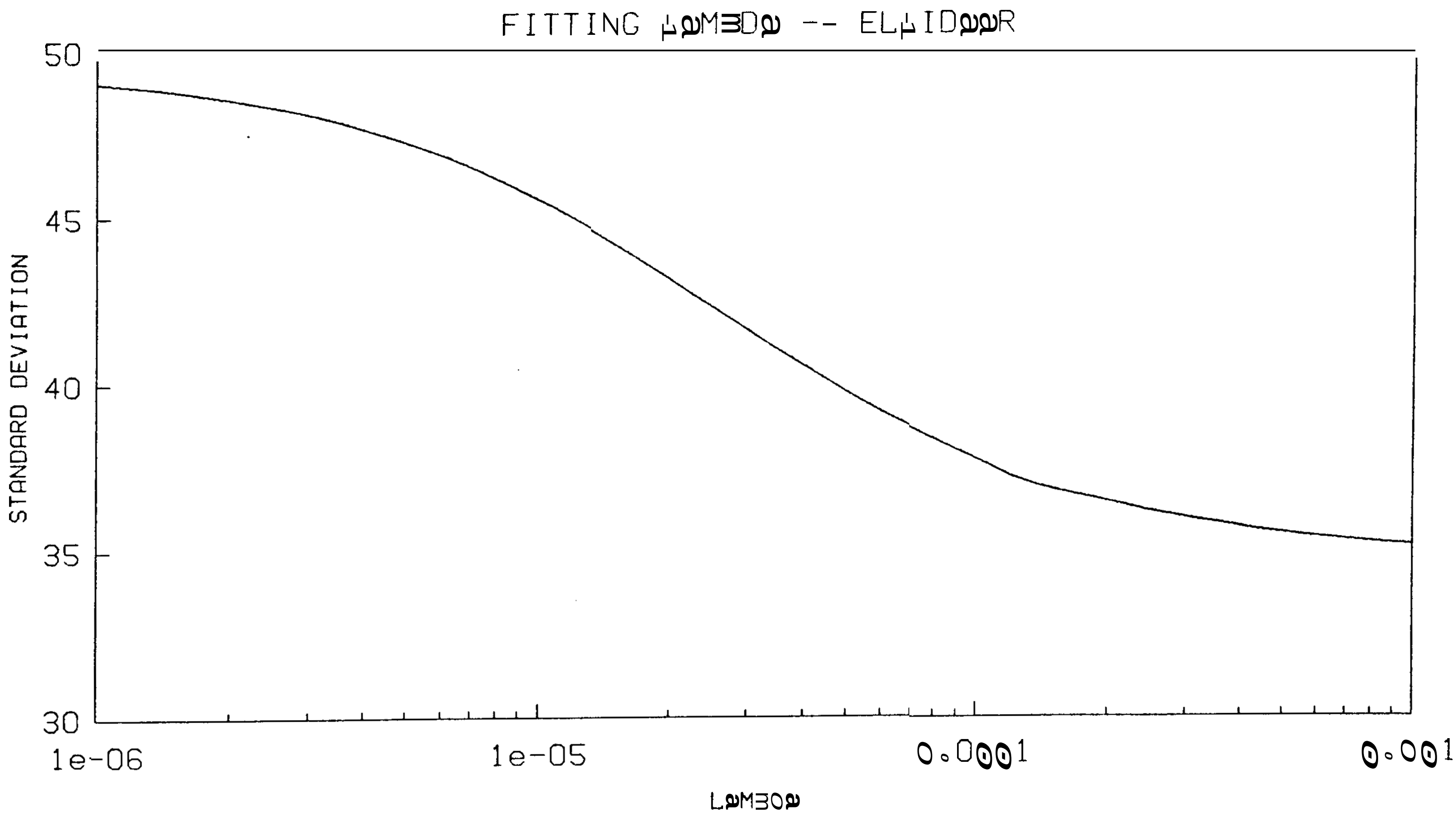

FIGURE-21. Standard deviation vs lambda (linear fit) for Ellidaar.

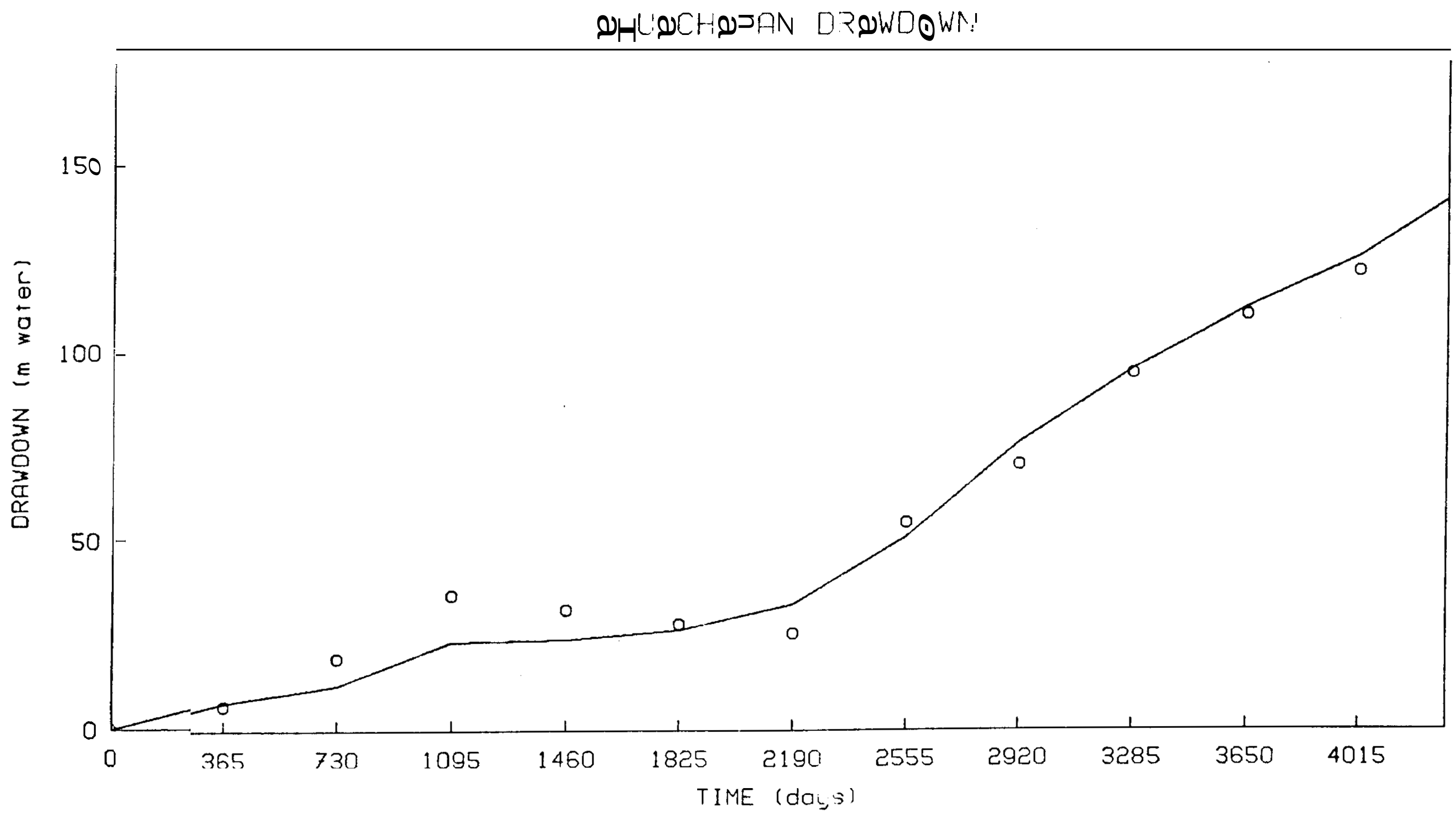

FIGURE-22. Radial match for Ahuachapan.

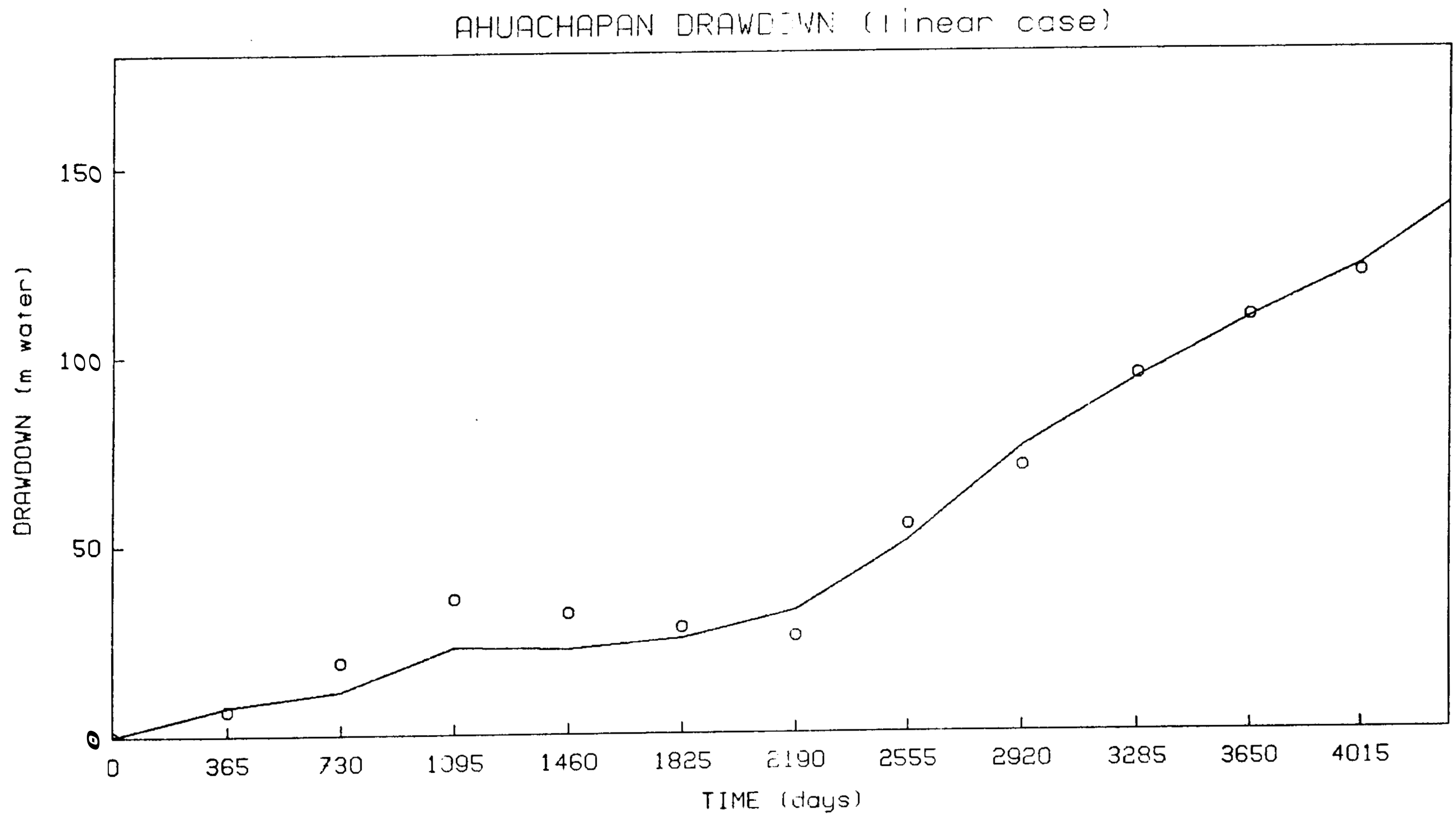

FIGURE-23. Linear match for Ahuachapan

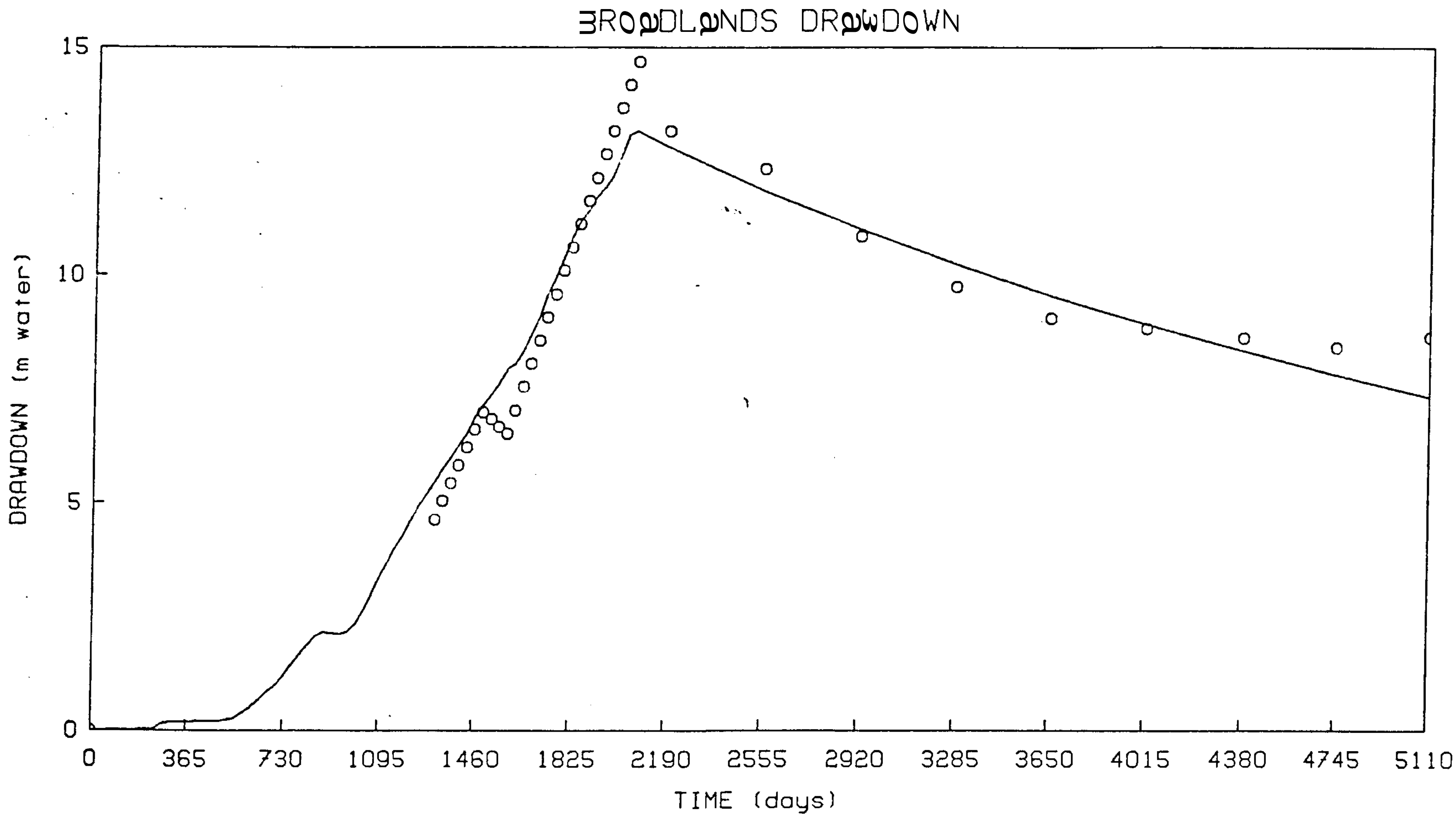

FIGURE-24. Radial match for Broadlands.

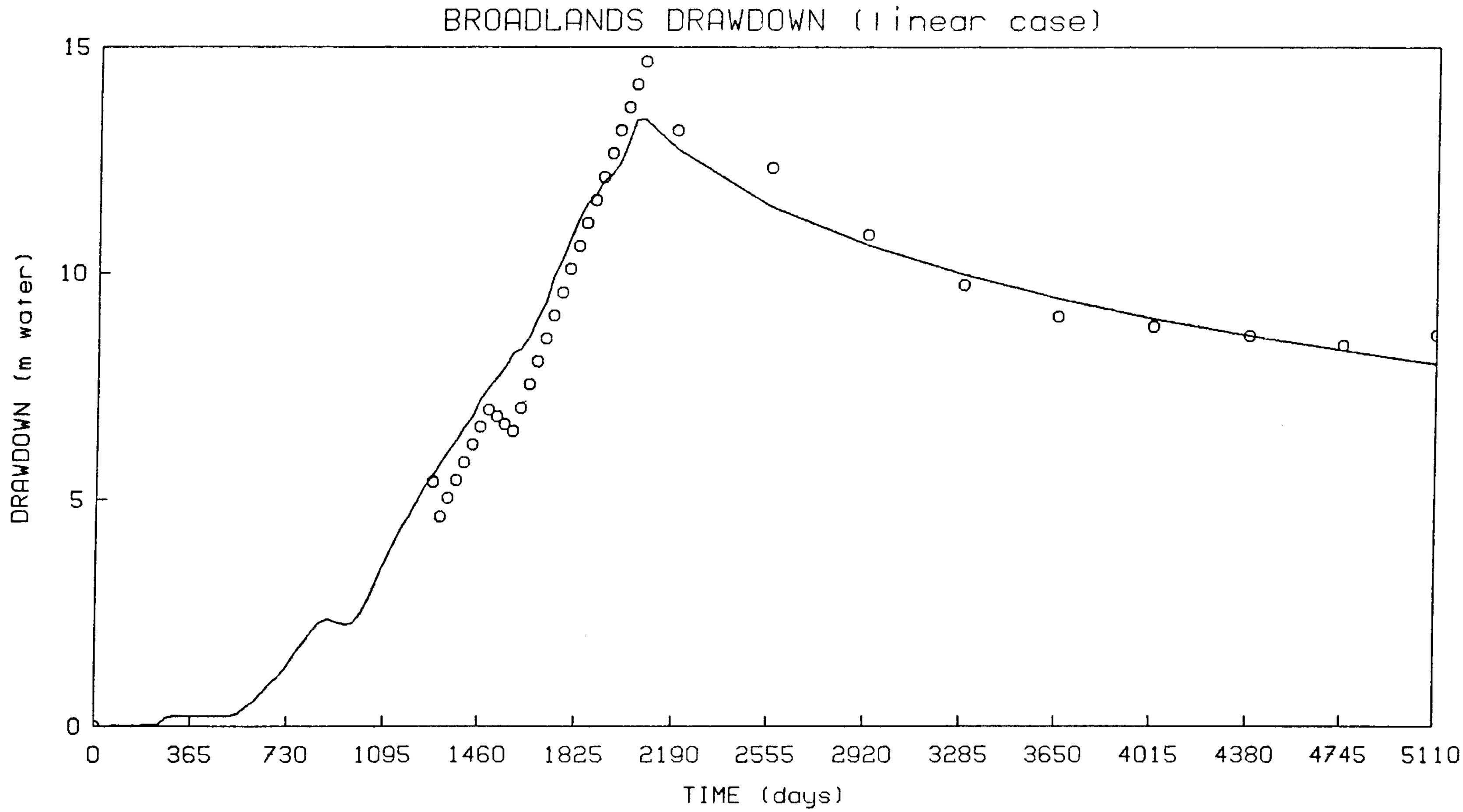

FIGURE-25. Linear match for Broadlands.

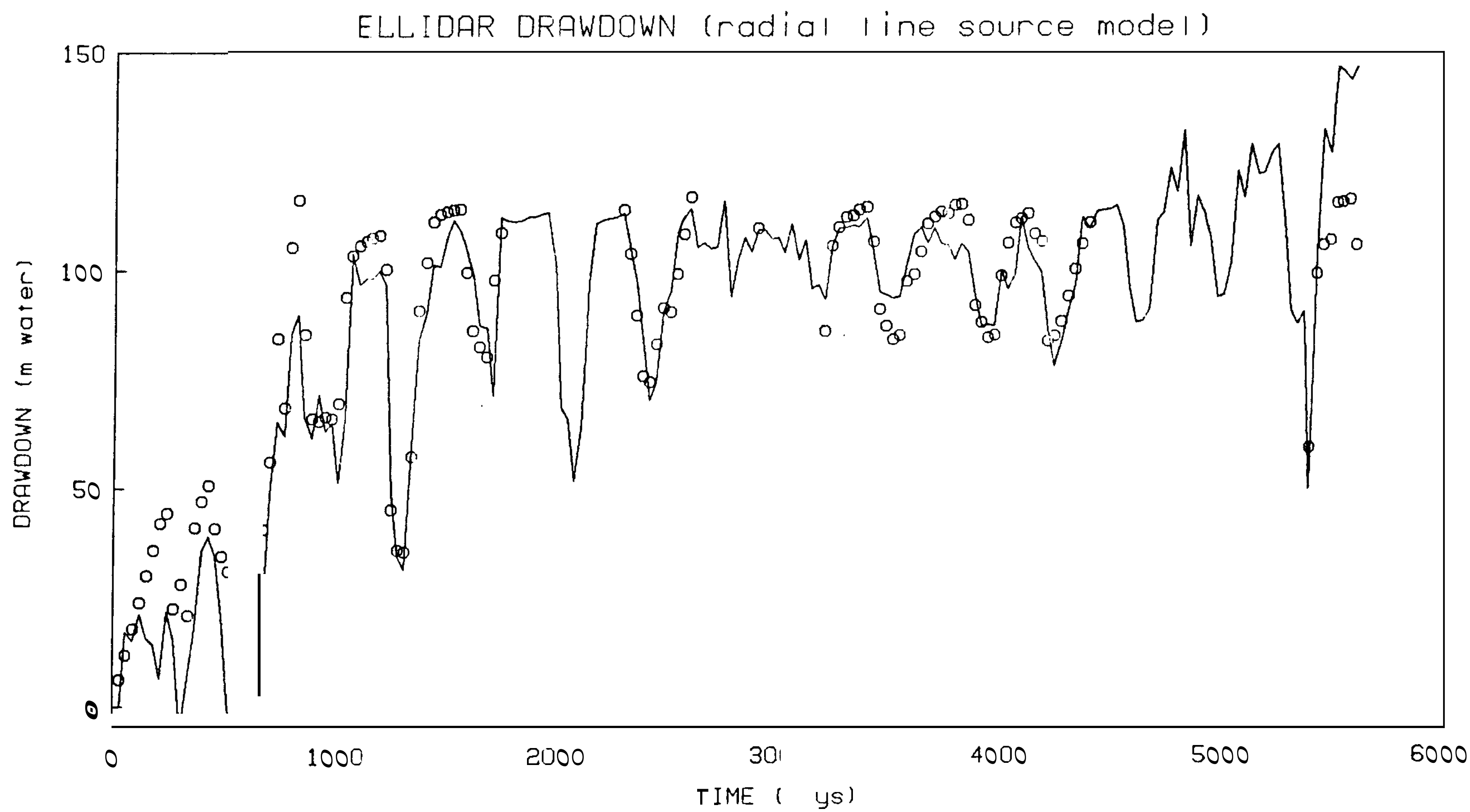

FIGURE-26. Radial (line source) match for Ellidaar.

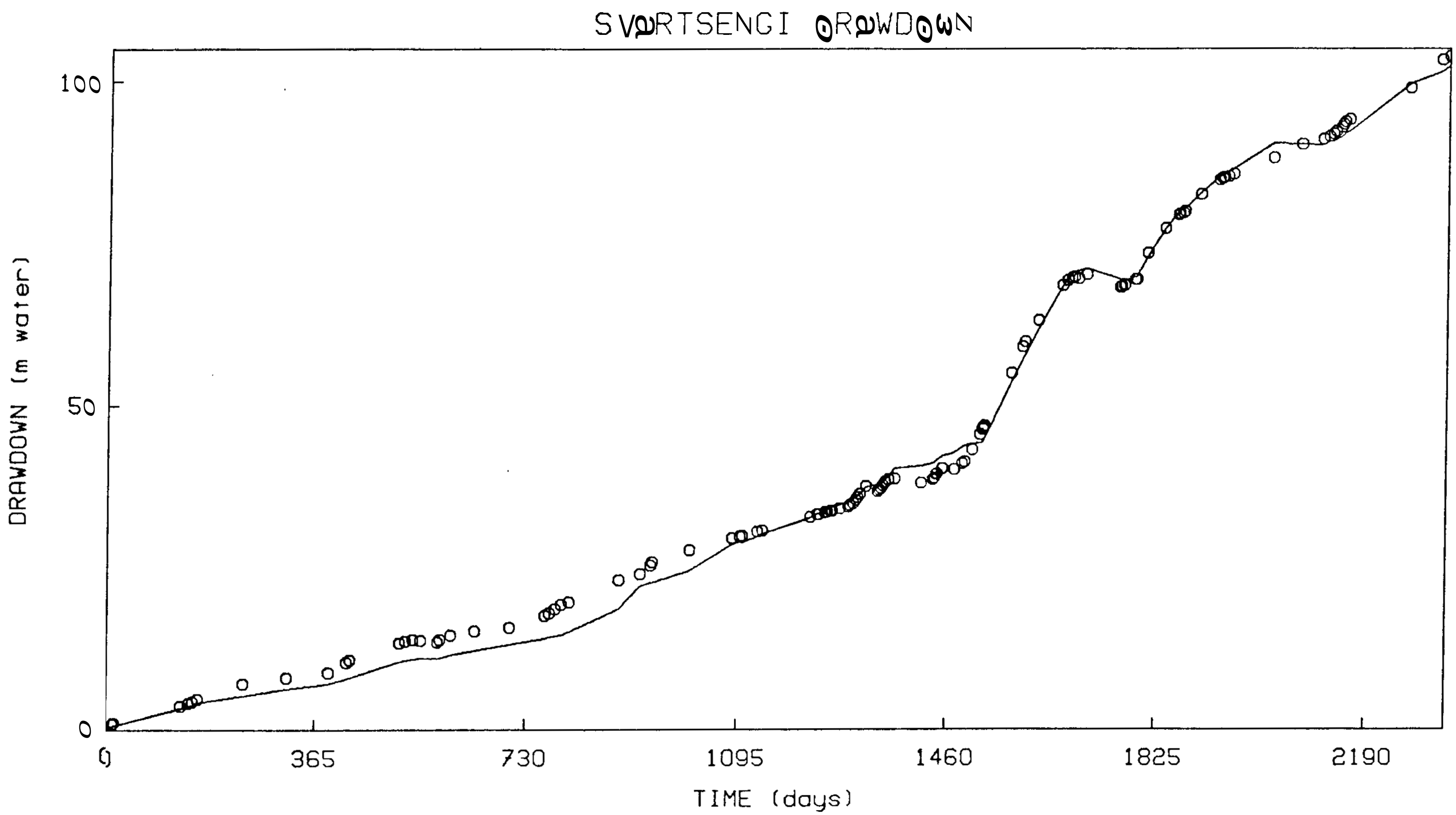

FIGURE-27. Radial match for Svartsengi

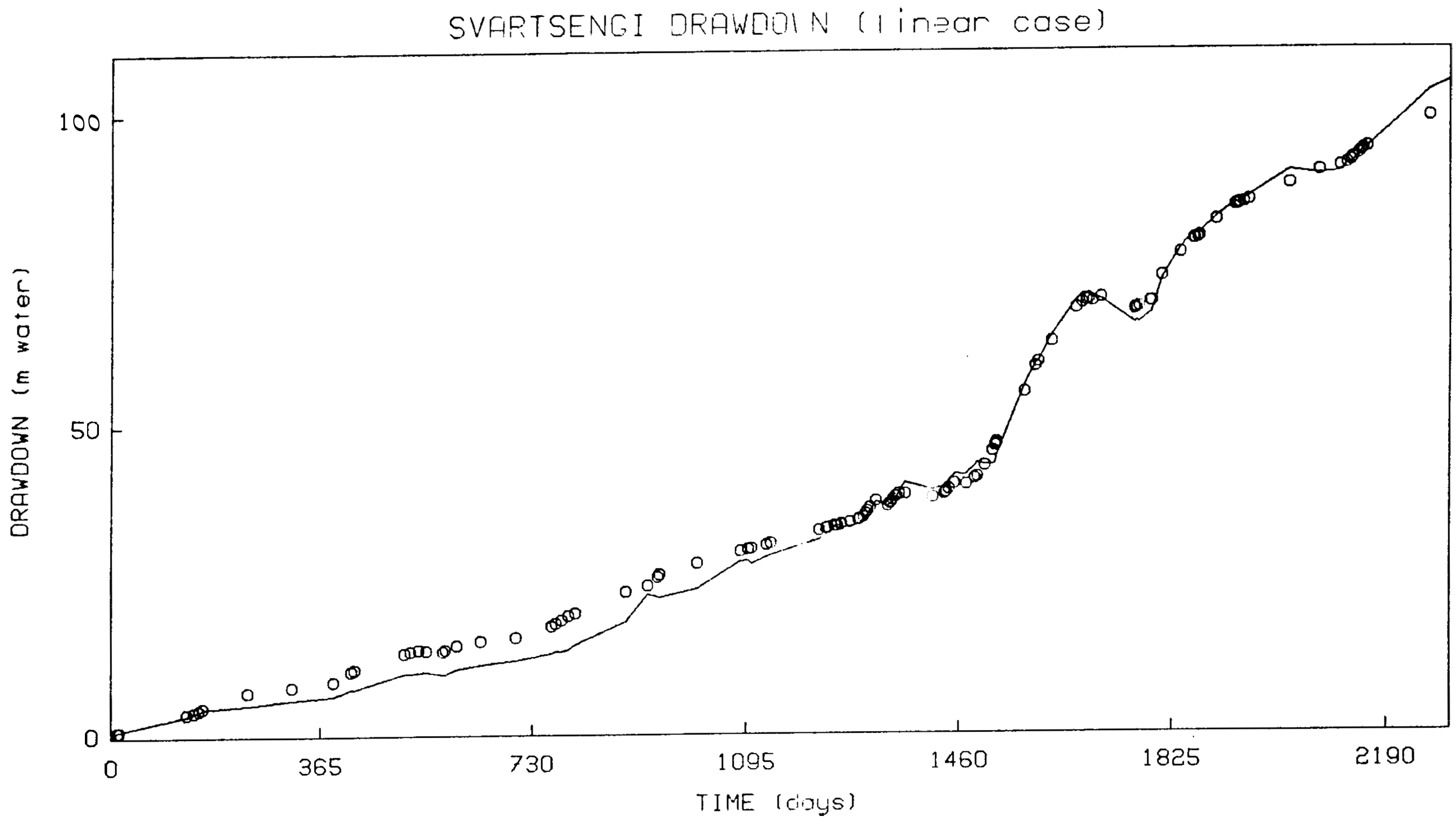

FIGURE 28. Linear match for Svartsengi

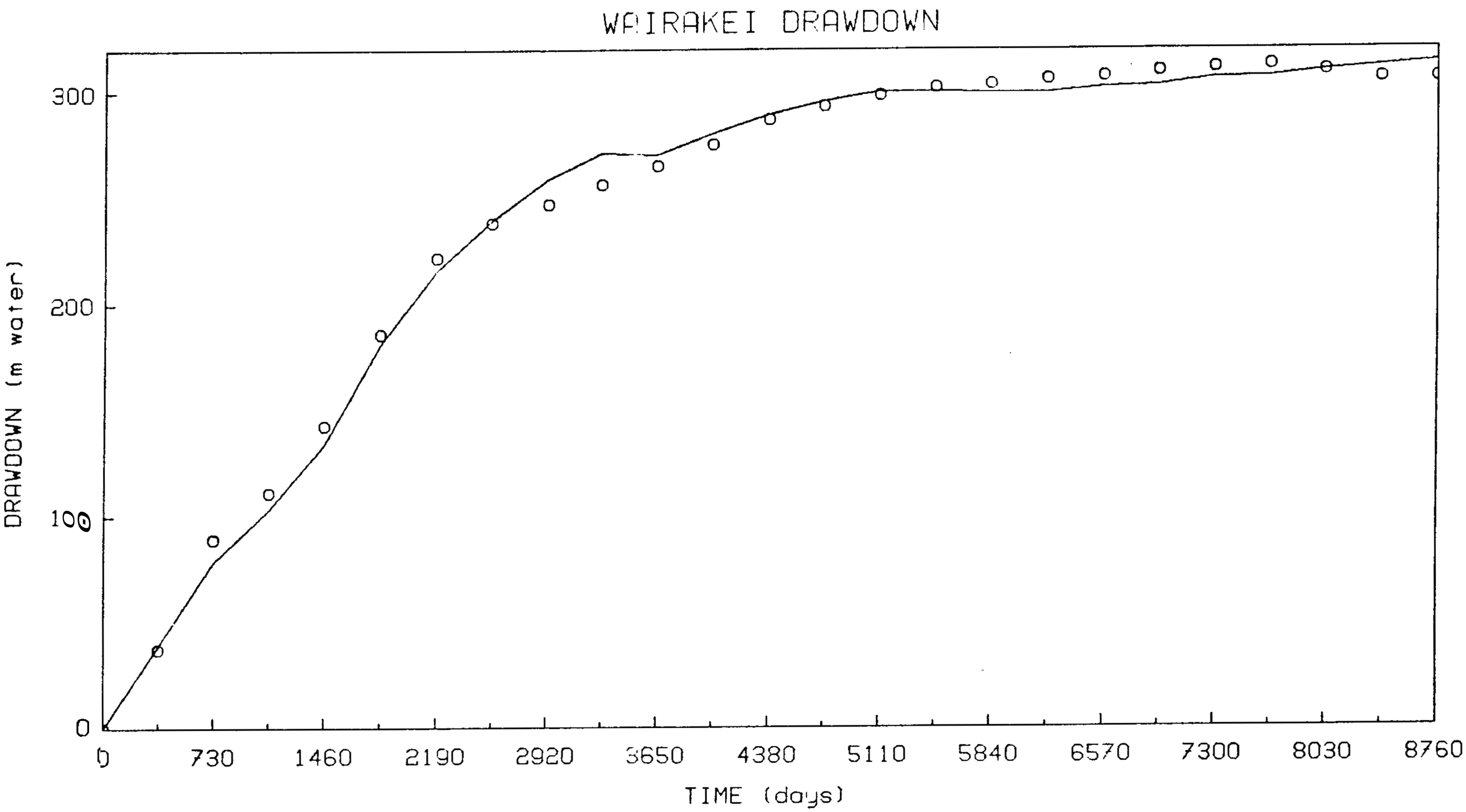

FIGURE-29. Radial match for Wairakei.

APPENDIX: Data Files and Computer Programs.

A 1. Data Files

The drawdown histories for the five fields are given in this section. They are presented in the format used by the programs: data triples, sets of time (in days), rate (kg/sec), and drawdown (m water). Their use with the programs is described in comment statements in the programs.

A2. The Computer Programs

The major programs used in this report are given here. Programs are written in FORTRAN 77 and were run under the UNIX operating system on the Stanford University Petroleum Engineering Department VAX 11/750 computer. Instructions for the programs are given as comments in the codes.

AHUACHAPAN

14

0.	0.	0
365.000	126.481	6.37105
730.000	105.939	19.1131
1095.00	240.947	35.6779
1460.00	90.3063	31.8552
1825.00	117.174	28.0326
2190.00	195.643	25.4842
2555.00	407.214	54.7910
2920.00	592.583	70.0816
3285.00	575,733	94.2915
3650.00	575.920	109.582
4015.00	564.228	121.050
4380.00	698.947	145.260
4745.00	550.298	156.728

WAIRAKEI

25

0.	0.	0.
365.000	1184.00	37.0000
730.000	1517.00	89.2000
1095.00	1340.00	110.900
1460.00	1643.00	142.700
1825.00	2327.00	186.000
2190.00	2245.00	221.700
2555.00	2087.00	238.300
2929.00	2039.00	247.200
3285.00	1890.00	256.100
3650.00	1513.00	265.000
4015.00	1769.00	275.200
4380.00	1776.00	286.700
4745.00	1722.00	293.100
5110.00	1665.00	298.200
5475.00	1528.00	302.000
5840.00	1490.00	303.300
6205.00	1462.00	305.800
6570.00	1509.00	307.100
6935.00	1475.00	309.600
7300.00	1532.00	310.900
7665.00	1454.00	312.200
8030.00	1512.00	309.600
8395.00	1490.00	305.800
8760.00	1487.00	305.800

ELLIDAAR

184

31.0000	15.3120	6.14800
59.0000	43.3780	11.7000
90.0000	37.3970	17.8500
120.000	46.0110	23.8000
151.000	35.6220	29.9500
181.000	33.1230	35.8900
212.000	20.6540	42.0400
243.000	46.3070	44.2700
273.000	34.2300	22.3800
304.000	0.	28.0000
334.000	22.8200	20.8900
365.000	40.9550	41.0408.
396.000	67.7630	46.9600
424.000	70.0140	50.8100
455.000	60.3120	40.8000
485.000	36.7860	34.4000
516.000	3.45160	31.0500
546.000	3.45160	27.8100
577.000	7.06630	24.4600
608.000	8.87980	21.1100
638.000	17.6300	17.8600
669.000	43.8080	40.7100
699.000	88.6360	56.1000
730.000	110.190	84.4300
761.000	99.8840	68.5700
789.000	135.560	105.300
820.000	137.090	116.300
850.000	94.9800	85.3200
881.000	88.3020	66.0380
911.000	104.750	65.4000
942.000	89.3710	66.4000
973.000	92.8340	66.1200
1003.00	69.9660	69.5100
1034.00	95.1040	93.8400
1064.00	155.410	103.400
1095.00	137.280	105.800
1126.00	137.190	106.800
1154.00	135.180	107.500
1185.00	136.610	108.100
1215.00	129.930	100.400
1246.00	51.5830	45.0500
1276.00	34.0860	35.7300
1307.00	34.3730	35.5000
1338.00	83.3990	57.3780
1368.00	121.060	90.7700
1399.00	126.120	101.800
1429.00	141.380	111.200
1460.00	137.090	112.900
1491.00	145.390	113.500
1519.00	150.160	113.900
1550.00	144.050	114.000
1580.00	135.660	99.5100
1611.00	126.020	86.2700
1641.00	107.320	82.5700
1672.00	107.900	80.1200
1703.00	83.2940	97.8600
1733.00	152.260	108.600
1764.00	146.060	109.200
1794.00	143.580	109.700
1825.00	142.620	110.200
1856.00	143.100	110.700
1884.00	142.050	111.100
1915.00	142.150	111.700
1945.00	142.050	112.100
1976.00	122.490	112.700
2006.00	69.7660	113.200
2037.00	70.9490	113.700
2068.00	50.5240	114.200
2098.00	74.0110	114.700
2129.00	128.600	115.200
2159.00	146.440	115.700
2190.00	143.860	116.200
2221.00	142.340	116.700
2249.00	141.100	117.200
2280.00	141.670	113.800
2310.00	126.880	103.800
2341.00	114.480	89.6200
2371.00	94.6560	75.6700
2402.00	74.5260	74.3800
2433.00	84.8110	83.0600
2463.00	111.810	91.4600
2494.00	117.910	90.3600
2524.00	138.430	99.1400
2555.00	141.670	108.200
2586.00	142.340	116.700
2614.00	126.400	116.000
2645.00	128.790	115.300
2675.00	126.210	114.600
2706.00	126.600	113.900
2736.00	143.480	113.200
2767.00	106.280	112.500
2798.00	122.490	111.800
2828.00	130.130	111.100
2859.00	123.830	110.300
2889.00	131.940	109.700
2920.00	131.080	107.700
2951.00	126.980	105.000
2979.00	127.550	102.600
3010.00	121.630	99.9200
3040.00	132.890	97.3400
3071.00	118.300	94.6600
3101.00	126.690	92.0800
3132.00	107.990	89.4100
3163.00	110.950	86.7400
3193.00	105.510	85.9300
3224.00	126.120	105.500
3254.00	131.650	109.900

FILLIDAAR CONT'D

3285.00	130.890	112.200
3316.00	130.700	112.600
3344.00	129.930	113.900
3375.00	132.700	114.400
3405.00	119.350	106.600
3436.00	104.940	91.0000
3466.00	105,700	87.1400
3497.00	105.320	84.0800
3528.00	106.660	85.0000
3558.00	119.250	97.5000
3589.00	129.270	99.0000
3619.00	130.320	104.200
3650.00	123.450	110.500
3681.00	128.890	112.100
3709.00	122.300	113.300
3740.00	122.020	113.000
3770.00	116.390	114.900
3801.00	122.880	115.000
3831.00	119.540	111.400
3862.00	103.320	91.7100
3893.00	93.6450	87.9100
3923.00	95.5910	84.4500
3954.00	95.9720	85.0000
3984.00	117.530	98.6700
4015.00	108.570	106.200
4046.00	114.770	110.800
4074.00	135.470	111.800
4105.00	121.730	112.900
4135.00	116.480	108.300
4166.00	112.480	106.600
4196.00	91.3260	83.6200
4227.00	80.0690	84.8800
4258.00	91.0690	88.1200
4288.00	102.940	94.0200
4319.00	112.570	100.100
4349.00	136.140	106.000
4380.00	129.270	110,700
4411.00	134.610	109.900
4439.00	133.940	108.400
4470.00	133.460	106.800
4500.00	134.040	105.200
4531.00	125.830	103.600
4561.00	102.460	102.000
4592.00	92.1280	100.400
4623.00	94.7700	98.8100
4653.00	100.070	97.2400
4684.00	133.080	95.6300
4714.00	134.040	94.0600
4745.00	148.350	92.4400
4776.00	137.190	90.8300
4804.00	159.990	89.3700
4835.00	114.100	87.7500
4865.00	135.090	86.1800
4896.00	128.120	84.5600
4926.00	118.870	83.0000
4957.00	97.4030	81.3800
4988.00	101.120	79.7600
5018.00	113.530	78.2000
5049.00	147.580	76.5800
5079.00	134.320	75.0200
5110.00	153.400	73.4000
51'41.00	140.140	71.7800
5169.00	140.520	70.3200
5200.00	147.110	68.7000
5230.00	149.210	67.1400
5261.00	119.250	65.5200
5291.00	88.1970	63.9500
5322.00	87.5100	62.3400
5353.00	93.9690	60.7200
5383.00	29.0490	59.1500
5414.00	123.920	98.8800
5444.00	165.040	105.500
5475.00	150.640	106.800
5506.00	180.590	115.200
5534.00	174.960	115.400
5565.00	169.140	116.100
5595.00	173.340	105.600

BROADLANDS

66

0.	0.	0.
243.3	2.949	1.029
273.7	94.80	1.157
304.2	23.59	1.286
486.7	4.820	2.057
517.1	4.566	2.186
547.5	33.88	2.314
577.9	96.61	2.443
608.3	97.02	2.571
638.7	124.9	2.700
669.2	149.1	2.829
699.6	112.6	2.957
730.0	163.2	3.086
760.4	198.7	3.214
790.8	184.3	3.343
821.3	194.7	3.471
851.7	159.0	3.600
882.1	83.32	3.729
912.5	0.	3.857
942.9	0.	3.986
973.3	31.96	4.114
1004.	168.1	4.243
1034.	223.5	4.372
1065.	311.1	4.500
1095.	295.4	4.629
1125.	295.8	4.757
1156.	265.0	4.886
1186.	252.0	5.014
1217.	263.7	5.143
1247.	296.6	5.271
1278.	231.1	5.400
1308.	239.5	4.616
1338.	239.1	5.031
1369.	234.1	5.428
1399.	252.0	5.826
1430.	233.8	6.222
1460.	324.0	6.619
1490.	255.5	6.993
1521.	225.0	6.827
1551.	227.7	6.660
1582.	286.1	6.520
1612.	145.1	7.030
1643.	261.9	7.540
1673.	339.2	8.049
1703.	343.8	8.559
1734.	449.3	9.069
1764.	345.7	9.580
1795.	377.3	10.09
1825.	424.5	10.60
1855.	318.7	11.11
1886.	254.7	11.62
1916.	296.6	12.13
1947.	228.8	12.64
1977.	252.4	13.15
2008.	408.1	13.66
2038.	435.2	14.17
2068.	151.1	14.68
2190.	0.	13.15
2555.	0.	12.33
2920.	0.	10.85
3285.	0.	9.741
3650.	0.	9.046
4015.	0.	8.828
4380.	0.	8.611
4745.	0.	8.407
5110.	0.	8.629

SVARTSENGI

123

0.	0.	0.
12.00	48.00	0.90
14.00	30.00	0.95
15.00	5.00	0.97
133.00	30.00	3.59
146.00	45.00	3.98
154.00	30.00	4.26
162.00	58.00	4.62
241.00	30.00	7.05
317.00	31.00	7.94
388.00	30.00	8.68
419.00	51.00	10.38
424.00	30.00	10.67
510.00	57.00	13.30
520.00	48.00	13.60
534.00	45.00	13.84
547.00	45.00	13.76
576.00	30.00	13.50
580.00	30.00	13.80
600.00	56.00	14.50
641.00	52.00	15.19
702.00	48.00	15.72
764.00	53.00	17.54
771.00	71.00	17.95
781.00	50.00	18.54
792.00	55.00	19.18
804.00	85.00	19.61
890.00	90.00	23.07
927.00	155.00	23.99
945.00	95.00	25.33
948.00	65.00	25.85
1012.00	95.00	27.61
1086.00	130.00	29.44
1099.00	115.00	29.76
1104.00	50.00	29.88
1130.00	115.00	30.52
1138.00	121.00	30.72
1223.00	115.00	32.82
1234.00	137.00	33.09
1235.00	131.00	33.11
1237.00	138.00	33.16
1248.00	161.00	33.44
1250.00	147.00	33.49
1251.00	134.00	33.51
1252.00	115.00	33.53
1258.00	125.00	33.68
1260.00	60.00	33.73
1274.00	110.00	34.08
1288.00	116.00	34.40
1292.00	131.00	34.58
1297.00	161.00	34.92
1302.00	151.00	35.40
1305.00	168.00	35.82
1309.00	188.00	36.36
1319.00	211.00	37.55
1339.00	116.00	36.71
1343.00	140.00	37.01
1345.00	150.00	37.21
1348.00	171.00	37.58
1353.00	186.00	38.11
1358.00	205.00	38.54
1368.00	226.00	38.64
1415.00	116.00	38.03
1435.00	120.00	38.57
1437.00	164.00	38.71
1438.00	163.00	38.79
1442.00	175.00	39.29
1443.00	183.00	39.43
1451.00	186.00	40.24
1452.00	192.00	40.22
1453.00	209.00	40.19
1472.00	129.00	40.11
1473.00	164.00	40.14
1487.00	172.00	41.04
1491.00	202.00	41.28
1504.00	129.00	43.15
1517.00	129.00	45.51
1521.00	135.00	46.23
1523.00	339.00	46.60
1524.00	279.00	46.78
1571.00	326.00	54.95
1590.00	344.00	59.07
1595.00	294.00	59.76
1618.00	347.00	63.02
1660.00	342.00	68.44
1669.00	336.00	69.24
1676.00	274.00	69.65
1681.00	280.00	69.83
1688.00	218.00	69.52
1702.00	222.00	70.11
1761.00	149.00	68.20
1762.00	152.00	68.25
1764.00	214.00	68.33
1768.00	149.00	68.50
1769.00	152.00	68.55
1787.00	206.00	69.37
1789.00	212.00	69.42
1790.00	272.00	69.44
1808.00	360.00	73.44
1839.00	341.00	77.21
1862.00	322.00	79.40
1864.00	273.00	79.46
1869.00	269.00	79.61
1872.00	249.00	79.86
1901.00	301.00	82.49
1932.00	299.00	84.73
1937.00	245.00	84.96
1940.00	299.00	85.10
1947.00	275.00	85.25
1956.00	281.00	85.63
2025.00	284.00	88.16
2075.00	224.00	90.30
2111.00	219.00	91.03
2122.00	269.00	91.44
2129.00	230.00	91.82
2133.00	280.00	92.20
2143.00	271.00	92.90
2146.00	311.00	93.28
2150.00	315.00	93.62
2157.00	263.00	94.02
2265.00	308.00	98.91
2319.00	283.00	103.30
2331.00	328.00	103.83

```
cccccccccccccccccccccccccccccccccccccccccccccccccccccccccccccc
c
c       hsl
c
c       Revised form of program hursimplin (Olsen, 1985)
c
c       This program is used to find the standard deviation and "slope'
c       term in the hurst simplified linear analysis, for a given value
c       of the Hurst parameter lambda.
c
c       USING THE PROGRAM:
c       The object is to find the lambda which minimizes the standard
c       deviation.  The method used here was to automize the following steps:
c       (On the UNIX system, a c-shell program did the following)
c       Create an input file of lambdas, in increasing order
c       Run hsl
c       Find lambda corresponding to minimum std. deviation
c       Make new file of lambdas ranging above and below the above sigma
c       Repeat to desired accuracy.
c       INPUT:
c       "t.q.dh" contains the field data of time, production, and drawdown.
c       The first line is the number of data points, subsequent lines contain
c       time(days), production rate(kg/sec), and drawdown(meters of water).
c
c       "k.fi" contains the following parameters: permeability(sq. meters),
c       porosity(unitless), and area of field(sq. meters)
c
c       Input from the standard input is the value for lambda.  This value
c       is NOT prompted, as usually the program reads these lambdas from a
c       file of many lambda values.  The program contains a loop such that
c       if a file of lambdas is redirected into the standard Input, lambdas
c       will be read until the file is finished.  Note: after the last lambda
c       is read, the program will attempt to read the end of file, resulting
c       in possible error statements.  As this caused no problems with the
c       operating system used, extra code for stopping the data input was not
c       used.
c
c       OUTPUT:
c       output is made to standard output.  For each lambda input, the output
c       is lambda, standard deviation, and "slope".
c
c
cccccccccccccccccccccccccccccccccccccccccccccccccccccccccccccc
        program hsl
        implicit real(a-h,o-z)
        real k,mu,lam
        dimension x(350),t(350),w(350),d(350),dc(350),cum(350)
        open(unit=1,file='t.q.dh',status='old')
        open(unit=7,file='k.fi',status='old')
        rewind(unit=1)
c
        read(1,*) npts
        read(1,*) (t(i),w(i),d(i),i=1,npts)
```

```
      read(7,*) k,fi
      mu=110.e-6
      c=1.e-9
      tc=3600.*24.*k/(fi*mu*c)
400   continue
      cum(1)=0.
      read(5,*) lam
      do 200 n=2,npts
      xx=0.
      do 100 j=2,n
      time=(t(n)-t(j-1))*tc
      xx=xx+(w(j)-w(j-1))*f(lam,time)
100   continue
      x(n)=xx
      cum(n)=cum(n-1)+w(n)*(t(n)-t(n-1))*24.*3600.
200   continue
      x(1)=0.
      call lsq(npts,x,d,slope)
      tot=0.
      do 300 i=1,npts
      dc(i)=x(i)*slope
      tot=tot+(dc(i)-d(i))**2.
300   continue
      sd=sqrt(tot/float(npts-1))
      write(6,1) lam,sd,slope
1     format(3(g12.5,5x))
      go to 400
      stop
      end
c
c
c
      function f(d,td)
      f=(exp(d**2.*td)*erfc(d*td**.5)-1.+(2.*d*td**.5)/1.772454)/d**2.
      return
      end
```

```
cccccccccccccccccccccccccccccccccccccccccccccccccccccccccccc
c
c       hsrtab
c
c       Revised form of program 'hursradflt'  (Marcou, 1985)
c       The major revision is that a table lookup program is used for
c       evaluation of the Hurst function, greatly increasing execution
c       speed.
c
c       This program is used to find the standard deviation and "slope'
c       term in the hurst simplified radial analysis, for a given value
c       of the Hurst parameter sigma.
c
c       USING THE PROGRAM:
c       The object is to find the sigma which minimizes the standard
c       (On the UNIX system, a c-shell program did the following)
c       deviation.  The method used here was to automize the following steps:
c       Create an input file of sigmas, in increasing order
c       Run hsrtab
c       Find sigma corresponding to minimum std. deviation
c       Make new file or sigmas ranging above and below the above sigma
c       Repeat to desired accuracy.
c       INPUT:
c       "t.q.dh" contains the field data of time, production, and drawdown.
c       The first line is the number of data points, subsequent lines contain
c       time(days), production rate(kg/sec), and drawdown(meters of water).
c
c       "k.fi" contains the following parameters: permeability(sq. meters).
c       porosity(unitless), and area of field(sq. meters)
c
c        Input from the standard input is the value for sigma.  This value
c        is NOT prompted, as usually the program reads these sigmas from a
c        file of many sigma values.  The program contains a loop such that
c        if a file of sigmas is redirected into the standard input, sigmas
c        will be read until the file is finished.  Note: after the last sigma
c        is read, the program will attempt to read the end of file, resulting
c        in possible error statements.  A5 this caused no problems with the
c        operating system used, extra code for stopping the data input was not
c        used.
c
c        OUTPUT:
c        Output is made to standard output.  For each sigma input, the output
c        is sigma, standard deviation, and "slope".
c
c
         program hsr
         implicit real*8(a-h,o-z)
         real*8 k,mu
         dimension x(350),t(350),w(350),d(350),dc(350),cum(350)
     1   ,ttab(50),ftab(50)
         open(unit=1,file='t.q.dh',status='old')
         open(unit=7,file='k.fi',status='old')
         rewind(unit=1)
```

```
c
        read(1,*) npts
        read(1,*) (t(i),w(i),d(i),i=1,npts)
        read(7,*) k,fi,area
        r=(area/3.14159)**.5
        mu=110.d-6
        c=1.d-9
        tc=3600.*24.*k/(fi*mu*c*(r**2.))
 400    continue
        ngood=npts
        cum(1)=0.
        read(5,*) sig
c
c       The subroutine maktab creates a table of time vs. Hurst function
c       for the given sigma.
c
        call maktab(tc,t(npts),sig,ttab,ftab)
c
c       Perform Hurst analysis
c
        do 200 n=2,npts
        xx=0.
        do 100 j=2,n
        time=(t(n)-t(j-1))*tc
        call lookup(ttab,ftab,50,time,hf)
        xx=xx+(w(j)-w(j-1))*hf
 100    continue
        x(n)=xx*sig
        cum(n)=cum(n-1)+w(n)*(t(n)-t(n-1))*24.*3600.
 200    continue
        x(1)=0.
c
c       The subroutine lsq performs a least squares fit (constrained through
c       the origin).
c
        call lsq2(npts,x,d,slope)
c
c       Calculate drawdown and std. deviation
c
        tot=0.
        do 300 i=1,npts
        dc(i)=x(i)*slope
        if(d(i).lt.-1.) then
                ngood=ngood-1
                go to 300
        else
        tot=tot+(dc(i)-d(i))**2.
        end if
 300    continue
        sd=sqrt(tot/float(ngood-1))
c
c       Output sigma, std.dev., and slope.
c
        write(6,500) sig,sd,slope
```

```
 500    format(3(2x,g14.6))
c
c       return for new sigma
c
        go to 400
        stop
        end
```

```
c        hursgraphrad,  revised from Marcou(1985)
c
c        This program is used to generate the Hurst prediction, given
c        sigma and "slope".  The correct sigma and "slope" are found
c        using program hsrtab.
c
c        INPUT:
c        "t.q.dh": time, production rate, and drawdown, as described
c        in program hsrtab
c        "k.fi": permeability, poroslty, and reservoir area, as described
c        in program hsrtab
c        sigma and 'slope" are prompted inputs on the standard input.
c
c        OUTPUT:
c        "hsrpred.out" is the graph-routine-ready output
c        of drawdown vs time.
c
c        *****************************************************
c
c                        main program
c
c        *****************************************************
c
         implicit real*8(a-h,o-z)
         real*8 k,mu
         dimension t(225),q(225),dh(225),sum(225),dhc(225),cum(225)
         open (unit=3,file='t.q.dh',status='old')
         rewind (unit=3)
         open (unit=2,file='hsrpred.out')
         rewind (unit=2)
         open (unit=1,file='k.fi')
c
c        ************* input data ***************
c
c
         read (3,*) l
         read (3,*) (t(i),q(i),dh(i),i=1,l)
         read (1,*) k,fi,area
         r2=area/3.14159
         mu=11Ø.e-6
         c=1.e-9
         tc=864ØØ.*k/(fi*mu*c*r2)
         write (6,*) ' '
         write (6,*) ' '
         write (6,*) 'what is the value of sigma?'
         read (5,*) sig
         write (6,*) ' '
         write (6,*) ' '
         write (6,*) 'what is the slope?'
         read (5,*) slope
c
c        ************** initialize and laplace solution **************
```

```
c
      do 200 i=1,l
         if (i.eq.1) then
            n=10
            m=150
            sum(1)=0.0
            dhc(1)=0.0
            cum(1)=0.0
         else
              do 100 j=2,i    .
                 dtd=tc*(t(i)-t(j-1))
                 sum(i)=sum(i)+(q(j)-q(j-1))*sig*sigman(dtd,n,m,sig)
  100         continue
         cum(i)= cum(i-1) + (q(i)*(t(i)-t(i-1))*60.*60.*24.)
         end if
  200 continue
c
c
c     ************* calculate drawdown ****************
c
c
      do 300 i=1,l
         dhc(i)=slope*sum(i)
  300 continue
c
c
c     ************* write to file "graph.dhc" ************
c
c     ******** first write the calculated drawdown ******
c
      write (2,*) l
      do 400 i=1,l
         write (2,*) t(i),dhc(i)
  400 continue
c
c     ********** now write the actual drawdown **********
c
      write (2,*) l
      do 500 i=1,l
         write (2,*) t(i),dh(i)
  500 continue
      stop
      end
```

```
c       hslpred,  revised from Olsen(1985)
c
c       This program is used to generate the Hurst prediction, given
c       lambda and "slope".  The correct lambda and 'slope" are found
c       using program hsl.
c
c       INPUT:
c       "t.q.dh": time, production rate, and drawdown, as described
c       in program hsrtab
c       "k.fi": permeability, porosity, and reservoir area, as described
c       in program hsrteb
c       lambda and "slope" are prompted inputs on the standard input.
c
c       OUTPUT:
c       "hsrpred.out" is the graph-routine-ready output
c
c       The first series of points is actual data,
c       the second series is the calculated drawdown.
c
ccccccccccccccccccccccccccccccccccccccccccccccccccccccccccccccccccc
        program hslpred
        implicit real(a-h,o-z)
        real k,mu,lam
        dimension x(350),t(350),w(350),d(350),dc(350),cum(350)
        open(unit=1,file='t.q.dh',status='old')
        rewind(unit=1)
        open(unit=7,file='hslpred.out')
        rewind(unit=7)
        open(unit=8,file='k.fi',status='old')
        rewind(unit=8)
c
        read(8,*) k,fi
        write(6,*) 'Enter lambda'
        read(5,*) lam
        write(6,*) 'Enter slope'
        read(5,*) slope
        read(1,*) npts
        read(1,*) (t(i),w(i),d(i),i=1,npts)
        mu=110.e-6
        c=1.e-9
        tc=3600.*24.*k/(fi*mu*c)
        cum(1)=0.
        do 200 n=2,npts
        xx=0.
        do 100 j=2,n
        time=(t(n)-t(j-1))*tc
        xx=xx+(w(j)-w(j-1))*f(lam,time)
 100    continue
        x(n)=xx
        cum(n)=cum(n-1)+w(n)*(t(n)-t(n-1))*24.*3600.
 200    continue
        x(1)=0.
        do 300 i=1,npts
```

```
      dc(i)=x(i)*slope
 300  continue
      write(7,*) npts
      write(7,10) (cum(i),d(i),i=1,npts)
      write(7,*) npts
      write(7,10) (cum(i),dc(i),i=1,npts)
 10   format(2(3x,g12.5))
      stop
      end
c
c
c
      function f(d,td)
      f=(exp(d**2.*td)*erfc(d*td**.5)-1.+(2.*d*td**.5)/1.772454)/d**2.
      return
      end
```

```
cccccccccccccccccccccccccccccccccccccccccccccccccccccccccccccccc
c
c       Program hsrlss: Line source solution history match
c       See program hsr for general description, here there
c       is no input sigma.
c
cccccccccccccccccccccccccccccccccccccccccccccccccccccccccccccccc
        program hsrlss
        implicit real*8(a-h,o-z)
        real*8 k,mu
        dimension x(350),t(350),w(350),d(350),dc(350),cum(350)
        open(unit=1,file='t.q.dh'.status='old')
        open(unit=2,file='hsrpred.out')
        open(unit=7.file='k.fi',status='old')
        rewind(unit=1)
c
        read(1,*) npts
        ngood=npts
        read(1,*) (t(i),w(i),d(i),i=1,npts)
        read(7.*) k.fi.area
        r=(area/3.14159)**.5
        mu=110.d-6
        c=1 .d-9
        tc=3600.*24.*k/(fi*mu*c*(r**2.))
        cum(1)=0.
        do 200 n=2,npts
        xx=0.
        do 100 j=2,n
        time=(t(n)-t(j-1))*tc
        xx=xx+(w(j)-w(j-1))*pdlss(time)
  100   continue
        x(n)=xx
        cum(n)=cum(n-1)+w(n)*(t(n)-t(n-1))*24.*3600.
  200   continue
        x(1)=0.
        call lsq2(npts,x,d,slope)
        tot=0.
        do 300 i=1,npts
        dc(i)=x(i)*slope
        if(d(i).lt.-10.) then
                ngood=ngood-1
                go to 300
        else
        tot=tot+(dc(i)-d(i))**2.
        endif
  300   continue
        sd=sqrt(tot/float(ngood-1))
        write(6,*) 'SD        SLOPE'
        write(6,2) sd,slope
        write(2,*) npts
        write(2,2)(cum(i),dc(i),i=1,npts)
        write(2.*) npts
        write(2,2)(cum(i),d(i),i=1,npts)
  2     format(2(g12.5,5x))
```